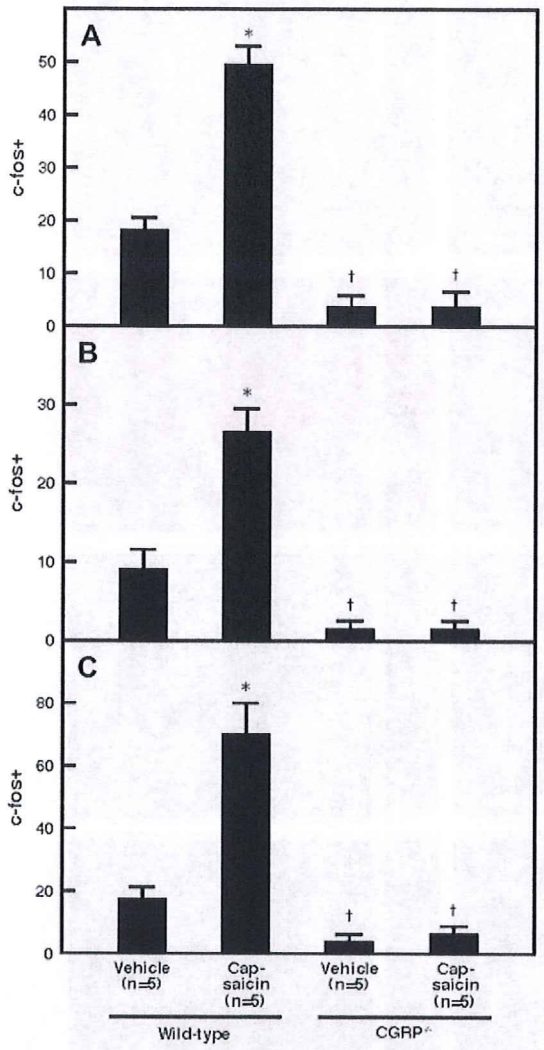

Fig 6. Effect of capsaicin administration on the number of *c-fos*-positive cells in the dorsal horn of spinal cord (**A**), medial brachial nucleus (**B**), and granular cell layer of the DG (**C**) in WT mice and CGRP–/– mice. The values are means ± SD derived from 5 animal experiments. $^{*}P < 0.01$ vs vehicle; $^{\dagger}P < 0.01$ vs WT.

The number of BrdU+/CD31+ cells, BrdU+/calbindin-D28K+ cells, and BrdU+/GFAP+ cells in the DG was significantly higher in WT mice than in CGRP–/– mice ($P < 0.01$) (Fig 8, *B–D*). A significant increase in the number of BrdU+/CD31+ cells (Fig 7, *A–F* and Fig 8, *B*) and BrdU+/calbindin-D28K+ cells (Fig 7, *G-L* and Fig 8, *C*), but not of BrdU+/GFAP+ cells (Fig 7, *M–R* and Fig 8, *D*), was observed in the DG increased at 30 min after administration of capsaicin in WT mice. In contrast, no increase in the number of any of these cells in the DG was observed after capsaicin administration in CGRP–/– mice (Fig 8, *B–D*).

Effect of capsaicin administration on spatial learning in WT and CGRP–/– mice. To determine whether capsaicin improves the cognitive function in mice by the stimulation of sensory neurons, we examined the effect of capsaicin administration on the spatial learning using the Morris water maze test for 8 consecutive days in WT and CGRP–/– mice. Capsaicin, IGF-I, or vehicle was administered only once 30 min before the trial on day 1. A CGRP receptor antagonist CGRP$^{8\text{-}33,38\text{-}41}$ and anti–IGF-I antibody was administered 30 min before the administration of capsaicin. In animals not administered capsaicin, a significant improvement of spatial learning was observed on days 3 to 8 as compared with that on day 1 in WT mice ($P < 0.02$) (Fig 9, *A*), whereas no improvement was noted throughout 8 days in CGRP–/– mice (Fig 9, *B*). In WT mice, capsaicin administration significantly enhanced the improvement of the spatial learning on days 3 to 8 as compared with that in the control animals not administered capsaicin (Fig 9, *A*). In contrast, capsaicin administration did not improve the spatial learning throughout the 8 days in CGRP–/– mice (Fig 9, *B*). Administration of CGRP$^{8\text{-}33,38\text{-}41}$ and anti–IGF-I antibody completely reversed the capsaicin-induced improvement of the spatial learning in WT mice (Fig 9, *A*). However, administration of IGF-I significantly improved the spatial learning on days 3 to 8 in both WT and CGRP–/– mice as compared with that in the control animals (Fig 9, *A* and *B*).

DISCUSSION

In the current study, we demonstrated that the hippocampal tissue levels of IGF-I and IGF-I mRNA were significantly lower in the CGRP–/– mice than in the WT mice. Capsaicin increased the hippocampal tissue levels of CGRP, IGF-I, and IGF-I mRNA, as well as the immunohistochemical expression of IGF-I at 30 min after the subcutaneous administration in WT mice but not in CGRP–/– mice. These observations strongly suggest that capsaicin might induce the transcription and production of IGF-I in the hippocampus by increasing the hippocampal CGRP levels. Consistent with this notion is our finding in a previous study demonstrating that the subcutaneous administration of capsaicin induced the transcription and production of IGF-I production in various tissues such as liver and kidneys by increasing the CGRP levels at 30 min after capsaicin administration.[15]

IGF-I immunoreactivity was colocalized with immunoreactivity for the astrocyte marker GFAP in the DG of WT mice given capsaicin. This observation is consistent with previous reports showing that astrocytes can produce IGF-I in the hippocampus.[19,38] CGRP has been shown to increase the cAMP levels via CGRP receptor activation in astrocytes.[39] Because cAMP plays an important role in IGF-I production,[20] it is possible

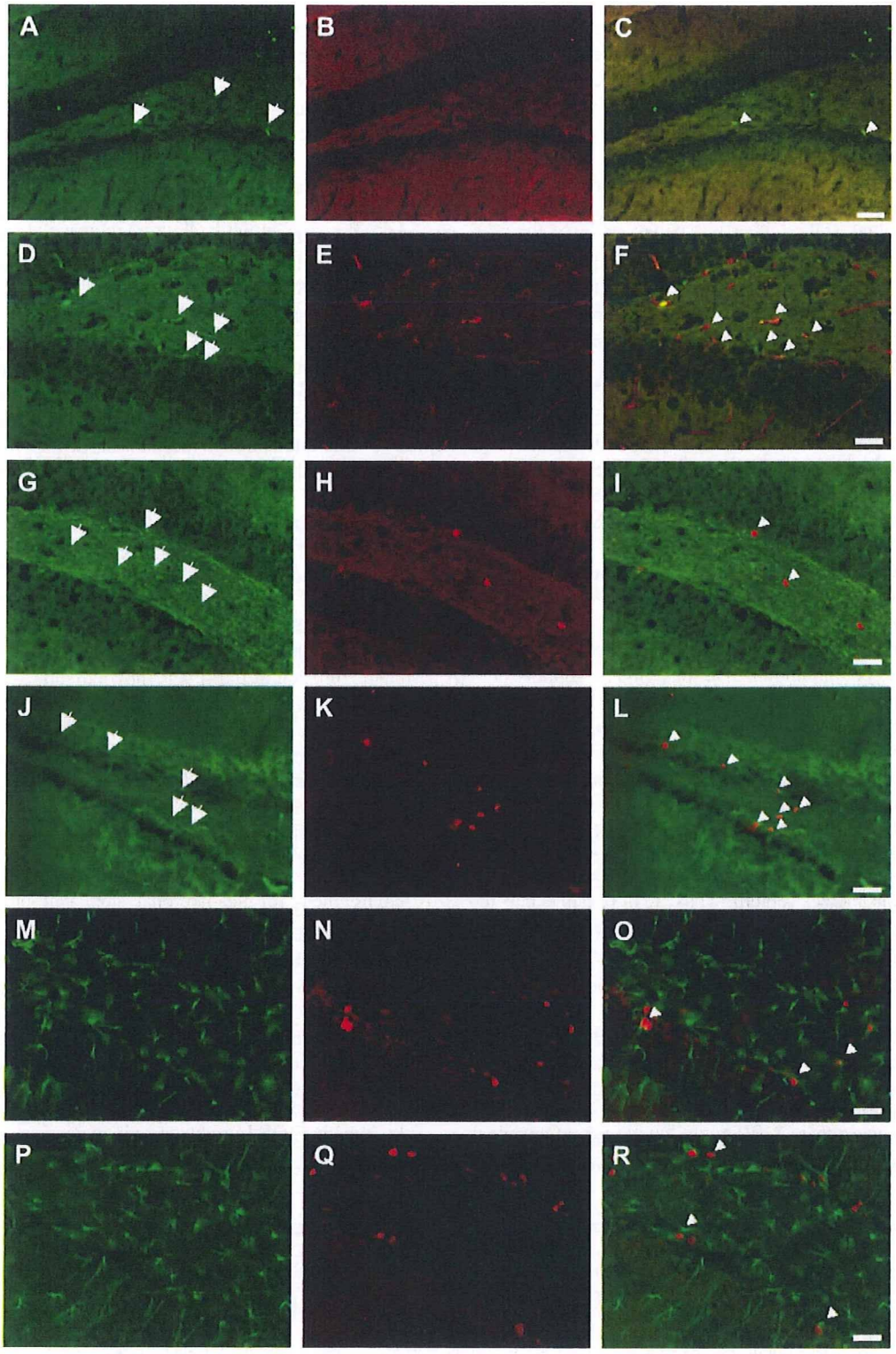
A
B
C
D
E
F
G
H
I
J
K
L
M
N
O
P
Q
R

that the stimulation of sensory neurons increases the CGRP levels in the hippocampus, which thereby increases IGF-I production via inducing an increase of the cAMP levels in the astrocytes. However, precisely which cells produce CGRP in the hippocampus of WT mice given capsaicin is not yet clear.

To examine the mechanism(s) by which sensory afferent information arising from capsaicin stimulation is transmitted to the hippocampus, we analyzed the *c-fos* expression in the spinal and supraspinal nervous tissues in WT and CGRP–/– mice after administration of capsaicin. In WT mice, an increase of *c-fos* expression was observed in the dorsal horn (lamina I-II) of the spinal cord and, supraspinally, in the parabrachial nuclei and the hippocampus after capsaicin administration. These observations strongly suggest that nociceptive information arising from stimulation with capsaicin may be transmitted to the hippocampus via the spinoparabrachial circuits. Consistent with this notion are observations in a previous report demonstrating that nociceptive information from the periphery and the spinal cord is transmitted to the limbic system including the hippocampus via the spinothalamic tract-parabrachial area-medial septum pathway or the thalamus.[40,41]

Nonprincipal neurons in the mouse hippocampus have been shown to be immunoreactive for CGRP.[17] Hippocampal nonprincipal neurons are innervated by GABAergic neurons projecting from the medial septum.[42] Because the medial septum receives sensory input from the parabrachial nuclei where the spinothalamic tracts terminate,[41] the increase in hippocampal tissue CGRP levels in WT mice given capsaicin might be a consequence of activation of the hippocampal nonprincipal neurons by GABAergic neurons projecting into them from the medial septum. Thus, it is possible that the CGRP released from the hippocampal nonprincipal neurons acts on astrocytes via the CGRP receptor to increase IGF-I production in the hippocampus in WT mice given capsaicin.

In contrast to the observations in WT mice given capsaicin, no increase in *c-fos* expression was observed in either the spinal or supraspinal nervous tissues after capsaicin administration in CGRP–/– mice. These observations suggest that CGRP might function as a transmitter in this sensory nervous relay system that leads to an increase in the hippocampal IGF-I production. Consistent with this hypothesis are previous reports demonstrating that CGRP is found in the synaptic contact regions between the primary afferent sensory neurons and spinothalamic tract neurons in the dorsal horn of the spinal cord,[43] in spinothalamic tract cells,[44] and in nerve fibers originating from the parabrachial nuclei.[13]

The numbers of CD31+, calbindin-D28K+, and GFAP+ cells in the BrdU-immunoreactive cells in the DG of the CGRP–/– mice were significantly lower than those in the WT mice, which suggests that CGRP and/or IGF-I might be closely involved in the proliferation of endothelial and neuronal stem cells in the mouse hippocampus. Consistent with this hypothesis is the previous report demonstrating that IGF-I is necessary for angiogenesis in the mouse adult brain[8] and for neuronal stem cell proliferation through mechanisms distinct from those of epidermal growth factor and fibroblast growth factor-2.[45]

Capsaicin administration increased the number of BrdU+ cells, that of BrdU+ and CD31+ cells, and that of BrdU+ and calbindin-D28K+ cells, but not of both BrdU+ and GFAP+ cells, in the DG of WT mice. In contrast, capsaicin administration had no effect on the number of these cells in the DG of CGRP–/– mice. A peripheral infusion of IGF-I was shown to induce angiogenesis selectively via a VEGF-dependent mechanism in the adult mouse brain[8] and neurogenesis in the adult rat hippocampus.[4] These observations strongly suggest that the stimulation of sensory neurons by capsaicin might induce angiogenesis and neurogenesis by inducing IGF-I production via an increase of the CGRP levels in the mouse hippocampus. Furthermore, because angiogenesis has been shown to offer a favorable environment for the neuronal stem cell proliferation via inducing the VEGF-dependent mechanism,[9] the hippocampal neurogenesis induced by capsaicin administration in WT mice might be mediated at least in part by angiogenesis.

IGF-I has been shown to have beneficial effects on the decline of cognitive function by inducing neurogenesis in the hippocampus,[4,46] which suggests that capsaicin administration might improve the cognitive function by inducing IGF-I production via increasing the CGRP levels in the mouse hippocampus. Consistent with this

Fig 7. Effect of capsaicin administration on the immunohistochemical expression of CD31, calbindin-D28 K, and BrdU in the hippocampus of WT mice. Fluorescent photomicrographs of cryostat sections showing the expression of CD31, calbindin-D28 K, or GFAP (green) in the hippocampi of WT mice were shown. Double labeling of either CD31 (**A** and **D**), calbindin-D28 K (**G** and **J**), or GFAP (**M** and **P**) and BrdU (**B, E, H, K, N,** and **Q**) were shown in the hippocampus. Vehicle (**A–C, G–I,** and **M–O**) or capsaicin (1 mg/kg) (**D–F, J–L,** and **P–R**) was injected subcutaneously, and tissues were removed 30 min after the vehicle or capsaicin injection. The arrows indicate IGF-I positive staining. The arrowheads indicate colocalization of IGF-I and GFAP positive staining. Five animals in each group were examined: typical results are shown. Scale bars = 25 μm.

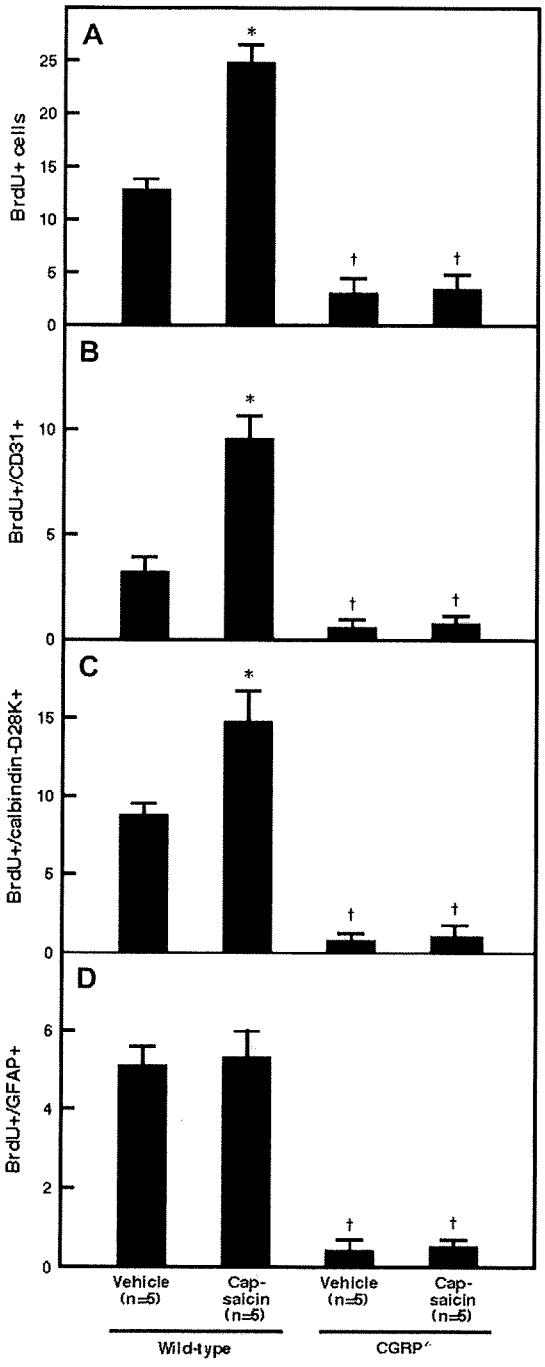

Fig 8. Effect of capsaicin administration on the hippocampal angiogenesis and neurogenesis in WT mice and CGRP–/– mice. All tissues were removed 30 min after subcutaneously injection of capsaicin (1 mg/kg) or vehicle. Values are expressed the means ± SD derived from 5 animal experiments. $^{*}P < 0.01$ vs vehicle; $^{\dagger}P < 0.01$ vs WT.

hypothesis are observations in the current study demonstrating that capsaicin administration significantly improved the spatial learning in WT mice but not in CGRP–/– mice. Pretreatment with an anti–IGF-I antibody reversed the improvement of the spatial learning in WT mice given capsaicin. The administration of IGF-I significantly improved the spatial learning in both WT mice and CGRP–/– mice. These observations suggest that the stimulation of sensory neurons by capsaicin might induce IGF-I production by increasing CGRP levels in the mouse hippocampus, which thereby improves the cognitive function.

In the current study, both angiogenesis and neurogenesis were observed at 30 min after administration of capsaicin. It is well known that it takes approximately 2 to 4 weeks before the newly generated neurons are functionally integrated and start modifying active hippocampal circuits.[45] IGF-I has been shown to exert critical enhancing effects on synaptic transmission and plasticity within minutes.[2] These observations suggest that the capsaicin-induced improvement of the cognitive function is mainly dependent on the latter effects induced by IGF-I in the mouse hippocampus.

Taken together, the observations in the current study strongly suggested that peripheral sensory nerve stimulation by capsaicin might increase the tissue levels of CGRP in the hippocampus, which thereby increases IGF-I production to produce improvement of the cognitive function in mice.

Of the various regulators of IGF-I production, GH is probably the most important, because it can exert its effects in both an endocrine and paracrine manner.[48] However, no decrease of IGF-I production in the brain was noted in GH receptor knockout mice.[47] These observations suggest that hippocampal or brain IGF-I production might be GH independent and that sensory neurons might at be involved at least in part in the GH-independent IGF-I production mechanism(s) in the hippocampus.

We previously reported that the pharmacologic stimulation of sensory neurons exerted therapeutic effects via inducing IGF-I production, which thereby prevented apoptosis via an increase in IGF-I production.[50] Neuronal death by apoptosis is implicated in the pathogenetic mechanisms of neurodegenerative diseases such as Alzheimer's disease,[49] which suggests that the pharmacologic stimulation of sensory neurons might ameliorate these pathologic conditions. Donepezil, which is one of therapeutic agents used clinically for Alzheimer's disease, has been shown to increase the serum levels of IGF-I in the elderly male,[36] which suggests that donepezil may stimulate sensory neurons, thereby contributing to improvement of cognitive function through the increase of IGF-I production in the hippocampus.

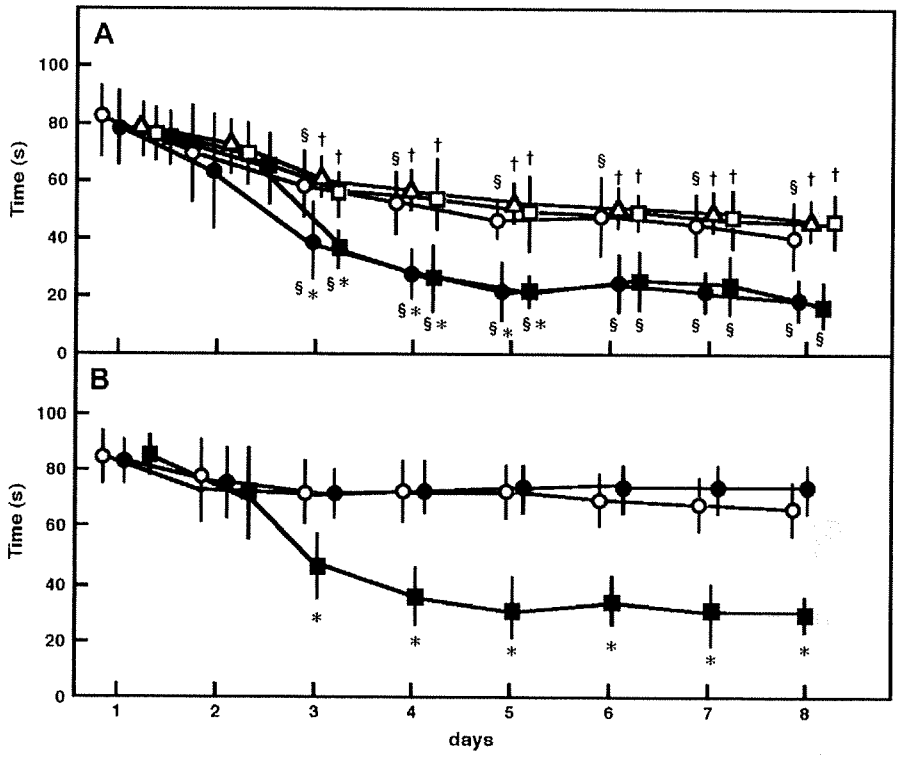

Fig 9. Effect of capsaicin administration on spatial learning in WT (**A**) and CGRP–/– (**B**) mice. Each value is expressed as the means ± SD derived from 10 animal experiments. **A**, Open circles, vehicle; closed circles, capsaicin; open triangles, capsaicin + CGRP (8-37); open squares, capsaicin + anti-IGF-I antibody; closed squares, IGF-I. **B**, Open circles, vehicle; closed circles, capsaicin; closed squares, IGF-I. $^{*}P < 0.01$ vs vehicle; $^{\dagger}P < 0.01$ vs capsaicin.

Consistent with this notion are observations in our recent study demonstrating that donepezil stimulates sensory neurons in the gastrointestinal tract to induce IGF-I production in the mouse hippocampus, which thereby contributes to improvement of cognitive function.[37]

REFERENCES

1. Daughaday WH, Rotwein P. Insulin-like growth factors I and II. Peptide, messenger ribonucleic acid and gene structures, serum, and tissue concentrations. Endocr Rev 1989;10:68–91.
2. Ramsey MM, Adams MM, Ariwodola OJ, Sonntag WE, Weiner JL. Functional characterization of des-IGF-1 action at excitatory synapses in the CA1 region of rat hippocampus. J Neurophysiol 2005;94:247–54.
3. Svensson J, Diez M, Engel J, et al. Endocrine, liver-derived IGF-I is of importance for spatial learning and memory in old mice. J Endocrinol 2006;189:617–27.
4. Aberg MA, Aberg ND, Hedbacker H, Oscarsson J, Eriksson PS. Peripheral infusion of IGF-I selectively induces neurogenesis in the adult rat hippocampus. J Neurosci 2000;20:2896–903.
5. Trejo JL, Llorens-Martin MV, Torres-Aleman I. The effects of exercise on spatial learning and anxiety-like behavior are mediated by an IGF-I-dependent mechanism related to hippocampal neurogenesis. Mol Cell Neurosci 2008;37:402–11.
6. Landi F, Capoluongo E, Russo A, et al. Free insulin-like growth factor-I and cognitive function in older persons living in community. Growth Horm IGF Res 2007;17:58–66.
7. Greenberg DA, Jin K. From angiogenesis to neuropathology. Nature 2005;438:954–9.
8. Lopez-Lopez C, LeRoith D, Torres-Aleman I. Insulin-like growth factor I is required for vessel remodeling in the adult brain. Proc Natl Acad Sci U S A 2004;101:9833–8.
9. Palmer TD, Willhoite AR, Gage FH. Vascular niche for adult hippocampal neurogenesis. J Comp Neurol 2000;425:479–94.
10. Maggi CA, Meli A. The sensory-efferent function of capsaicin-sensitive sensory neurons. Gen Pharmacol 1988;19:1–43.
11. Dray A. Inflammatory mediators of pain. Br J Anaesth 1995;75:125–31.
12. Rosenfeld MG, Emeson RB, Yeakley JM, et al. Calcitonin gene-related peptide: a neuropeptide generated as a consequence of tissue-specific, developmentally regulated alternative RNA processing events. Ann N Y Acad Sci 1992;657:1–17.
13. Dobolyi A, Irwin S, Makara G, Usdin TB, Palkovits M. Calcitonin gene-related peptide-containing pathways in the rat forebrain. J Comp Neurol 2005;489:92–119.
14. van Rossum D, Hanisch UK, Quirion R. Neuroanatomical localization, pharmacological characterization and functions of CGRP, related peptides and their receptors. Neurosci Biobehav Rev 1997;21:649–78.

15. Harada N, Okajima K, Kurihara H, Nakagata N. Stimulation of sensory neurons by capsaicin increases tissue levels of IGF-I, thereby reducing reperfusion-induced apoptosis in mice. Neuropharmacology 2007;52:1303–11.
16. Suzuki R, Morcuende S, Webber M, Hunt SP, Dickenson AH. Superficial NK1-expressing neurons control spinal excitability through activation of descending pathways. Nat Neurosci 2002;5: 1319–26.
17. Sakurai O, Kosaka T. Nonprincipal neurons and CA2 pyramidal cells, but not mossy cells are immunoreactive for calcitonin gene-related peptide in the mouse hippocampus. Brain Res 2007;1186:129–43.
18. Moreno MJ, Terron JA, Stanimirovic DB, Doods H, Hamel E. Characterization of calcitonin gene-related peptide (CGRP) receptors and their receptor-activity-modifying proteins (RAMPs) in human brain microvascular and astroglial cells in culture. Neuropharmacology 2002;42:270–80.
19. Ye P, Popken GJ, Kemper A, McCarthy K, Popko B, D'Ercole AJ. Astrocyte-specific overexpression of insulin-like growth factor-I promotes brain overgrowth and glial fibrillary acidic protein expression. J Neurosci Res 2004;78:472–84.
20. Vignery A, McCarthy TL. The neuropeptide calcitonin gene-related peptide stimulates insulin-like growth factor I production by primary fetal rat osteoblasts. Bone 1996;18:331–5.
21. Oh-hashi Y, Shindo T, Kurihara Y, et al. Elevated sympathetic nervous activity in mice deficient in alphaCGRP. Circ Res 2001;89: 983–90.
22. Harada N, Okajima K, Uchiba M, Katsuragi T. Ischemia/reperfusion-induced increase in the hepatic level of prostacyclin is mainly mediated by activation of capsaicin-sensitive sensory neurons in rats. J Lab Clin Med 2002;139:218–26.
23. Daemen MA, van 't Veer C, Denecker G, et al. Inhibition of apoptosis induced by ischemia-reperfusion prevents inflammation. J Clin Invest 1999;104:541–9.
24. Harada N, Okajima K, Uchiba M, Katsuragi T. Contribution of capsaicin-sensitive sensory neurons to stress-induced increases in gastric tissue levels of prostaglandins in rats. Am J Physiol Gastrointest Liver Physiol 2003;285:G1214–24.
25. Trejo JL, Carro E, Torres-Aleman I. Circulating insulin-like growth factor I mediates exercise-induced increases in the number of new neurons in the adult hippocampus. J Neurosci 2001;21:1628–34.
26. Standley PR, Obards TJ, Martina CL. Cyclic stretch regulates autocrine IGF-I in vascular smooth muscle cells: implications in vascular hyperplasia. Am J Physiol 1999;276:E697–705.
27. Liu L, Simon SA. Capsazepine, a vanilloid receptor antagonist, inhibits nicotinic acetylcholine receptors in rat trigeminal ganglia. Neurosci Lett 1997;228:29–32.
28. Sirotkin AV, Florkovicova I, Makarevich AV, et al. Oxytocin mediates some effects of insulin-like growth factor-I on porcine ovarian follicles. J Reprod Dev 2003;49:141–9.
29. Tomomasa T, Ogawa T, Hikima A, Tabata M, Kaneko H, Morikawa A. Developmental changes in cyclooxygenase mRNA expression in the gastric mucosa of rats. J Pediatr Gastroenterol Nutr 2002;34:169–73.
30. Bortz JD, Rotwein P, DeVol D, Bechtel PJ, Hansen VA, Hammerman MR. Focal expression of insulin-like growth factor I in rat kidney collecting duct. J Cell Biol 1988;107:811–9.
31. Linden AM, Greene SJ, Bergeron M, Schoepp DD. Anxiolytic activity of the MGLU2/3 receptor agonist LY354740 on the elevated plus maze is associated with the suppression of stress-induced c-Fos in the hippocampus and increases in c-Fos induction in several other stress-sensitive brain regions. Neuropsychopharmacology 2004;29:502–13.
32. Shukitt-Hale B, McEwen JJ, Szprengiel A, Joseph JA. Effect of age on the radial arm water maze-a test of spatial learning and memory. Neurobiol Aging 2004;25:223–9.
33. Savelieva KV, Rajan I, Baker KB, et al. Learning and memory impairment in Eph receptor A6 knockout mice. Neurosci Lett 2008; 438:205–9.
34. Sidman RL, Angevine JBJ, Pierce ET. Atlas of the mouse brain and spinal cord. Cambridge, MA: Harvard University Press, 1977.
35. Franklin KBJ, Paxinos G. The mouse brain in stereotaxic coodinates. New York: Academic Press, 1997.
36. Obermayr RP, Mayerhofer L, Knechtelsdorfer M, et al. The age-related down-regulation of the growth hormone/insulin-like growth factor-1 axis in the elderly male is reversed considerably by donepezil, a drug for Alzheimer's disease. Exp Gerontol 2005;40:157–63.
37. Narimatsu N, Harada N, Kurihara H, Nakagata N, Sobue K, Okajima K. Donepezil improves cognitive function in mice by increasing the production of insulin-like growth factor-I in the hippocampus. J Pharmacol Exp Ther. In press.
38. Hwang IK, Yoo KY, Park SK, et al. Expression and changes of endogenous insulin-like growth factor-1 in neurons and glia in the gerbil hippocampus and dentate gyrus after ischemic insult. Neurochem Int 2004;45:149–56.
39. Lazar P, Reddington M, Streit W, Raivich G, Kreutzberg GW. The action of calcitonin gene-related peptide on astrocyte morphology and cyclic AMP accumulation in astrocyte cultures from neonatal rat brain. Neurosci Lett 1991;130:99–102.
40. Klop EM, Mouton LJ, Hulsebosch R, Boers J, Holstege G. In cat four times as many lamina I neurons project to the parabrachial nuclei and twice as many to the periaqueductal gray as to the thalamus. Neuroscience 2005;134:189–97.
41. Castle M, Comoli E, Loewy AD. Autonomic brainstem nuclei are linked to the hippocampus. Neuroscience 2005;134:657–69.
42. Gulyas AI, Toth K, Danos P, Freund TF. Subpopulations of GABAergic neurons containing parvalbumin, calbindin D28k, and cholecystokinin in the rat hippocampus. J Comp Neurol 1991; 312:371–8.
43. Carlton SM, Westlund KN, Zhang DX, Sorkin LS, Willis WD. Calcitonin gene-related peptide containing primary afferent fibers synapse on primate spinothalamic tract cells. Neurosci Lett 1990; 109:76–81.
44. Tie-Jun SS, Xu Z, Hokfelt T. The expression of calcitonin gene-related peptide in dorsal horn neurons of the mouse lumbar spinal cord. Neuroreport 2001;12:739–43.
45. Arsenijevic Y, Weiss S, Schneider B, Aebischer P. Insulin-like growth factor-I is necessary for neural stem cell proliferation and demonstrates distinct actions of epidermal growth factor and fibroblast growth factor-2. J Neurosci 2001;21:7194–202.
46. Carro E, Torres-Aleman I. Serum insulin-like growth factor I in brain function. Keio J Med 2006;55:59–63.
47. Kitabatake Y, Sailor KA, Ming GL, Song H. Adult neurogenesis and hippocampal memory function: new cells, more plasticity, new memories? Neurosurg Clin N Am 2007;18:105–13. x.
48. Kopchick JJ, Andry JM. Growth hormone (GH), GH receptor, and signal transduction. Mol Genet Metab 2000;71:293–314.
49. Lupu F, Terwilliger JD, Lee K, Segre GV, Efstratiadis A. Roles of growth hormone and insulin-like growth factor 1 in mouse postnatal growth. Dev Biol 2001;229:141–62.
50. Harada N, Okajima K, Kurihara H, Nakagata N. Antithrombin prevents reperfusion-induced hepatic apoptosis by enhancing insulin-like growth factor-I production in mice. Crit Care Med 2008;36: 971–4.
51. Camins A, Pallas M, Silvestre JS. Apoptotic mechanisms involved in neurodegenerative diseases: experimental and therapeutic approaches. Methods Find Exp Clin Pharmacol 2008;30:43–65.

0022-3565/09/3301-2–12$20.00
THE JOURNAL OF PHARMACOLOGY AND EXPERIMENTAL THERAPEUTICS
Copyright © 2009 by The American Society for Pharmacology and Experimental Therapeutics
JPET 330:2–12, 2009

Vol. 330, No. 1
147280/3477029
Printed in U.S.A.

Donepezil Improves Cognitive Function in Mice by Increasing the Production of Insulin-Like Growth Factor-I in the Hippocampus

Noriko Narimatsu, Naoaki Harada, Hiroki Kurihara, Naomi Nakagata, Kazuya Sobue, and Kenji Okajima

Departments of Anesthesiology and Medical Crisis Management (N.Nar., K.S.) and Translational Medical Science Research (N.H., K.O.), Nagoya City University Graduate School of Medical Sciences, Nagoya, Japan; Department of Physiological Chemistry and Metabolism, University of Tokyo, Graduate School of Medicine, Tokyo, Japan (H.K.); and Division of Reproductive Engineering, Center for Animal Resources and Development, Kumamoto University, Kumamoto, Japan (N.Nak.)

Received October 13, 2008; accepted March 23, 2009

ABSTRACT

Insulin-like growth factor-I (IGF-I) exerts beneficial effects on cognitive function. The selective acetylcholinesterase inhibitor donepezil increases serum IGF-I levels in elderly subjects. Because stimulation of sensory neurons induces IGF-I production by releasing calcitonin gene-related peptide (CGRP) in the mouse brain, we hypothesized that donepezil increases IGF-I production by sensory neuron stimulation to improve the cognitive function in mice. Donepezil, but not tacrine, increased the CGRP release from dorsal root ganglion neurons isolated from wild-type (WT) mice. Pretreatment with the protein kinase A inhibitor KT5720 [(9*S*,10*S*,12*R*)-2,3,9,10,12-hexahydro-10-hydroxy-9-methyl-1-oxo-9,12-epoxy-1*H*-diindolo[1,2,3-fg:3′,2′,1′-kl]pyrrolo[3,4-i][1,6]-benzo-diazocine-10-carboxylic acid hexyl ester] reversed the effects induced by donepezil. Increase in tissue levels of CGRP, IGF-I, and IGF-I mRNA in the hippocampus was observed at 4 weeks after oral administration of donepezil in WT mice. In these animals, c-*fos* expression in spinal dorsal horns, parabrachial nuclei, the solitary tract nucleus, and the hippocampus was increased. Enhancement in angiogenesis and neurogenesis was observed in the dentate gyrus of the hippocampus of WT mice after donepezil administration. Improvement of spatial learning was observed in WT mice after donepezil administration. Oral administration of tacrine for 4 weeks produced none of the aforementioned effects induced by donepezil in WT mice. However, none of the effects observed in WT mice was seen after donepezil administration in CGRP-knockout mice and WT mice subjected to functional denervation. These observations suggest that donepezil may improve cognitive function in mice by increasing the hippocampal production of IGF-I through sensory neuron stimulation. These effects of donepezil may not be dependent on its acetylcholinesterase inhibitory activity.

Activation of the central cholinergic system has been shown to induce hippocampal neurogenesis, thereby contributing to improvement of cognitive function (Kotani et al., 2006). In this context, the selective acetylcholinesterase inhibitor donepezil has been reported to improve the cognitive impairment in Alzheimer's disease (Winblad et al., 2006).

Insulin-like growth factor-I (IGF-I) is a basic peptide composed of 70 amino acids, with ubiquitous distribution in various tissues and cells (Okajima and Harada, 2008). It mediates the growth-promoting actions of growth hormone (GH) and plays an important role in postnatal and adolescent growth (Okajima and Harada, 2008). IGF-I has been shown to enhance excitatory synaptic transmission in the CA_1 region of the hippocampus (Ramsey et al., 2005) and to improve spatial learning by inducing neurogenesis in the hippocampus (Aberg et al., 2000). The impaired spatial learning in mice with low serum levels of IGF-I is reversed by exogenous administration of IGF-I (Trejo et al., 2008). A close correlation has been shown between the plasma IGF-I levels, and cognitive function has been shown in older individuals (Landi et al., 2007). These observations strongly suggest that IGF-I may improve cognitive function by increasing the plasticity and promoting neurogenesis in the hippocampus.

Article, publication date, and citation information can be found at http://jpet.aspetjournals.org.
doi:10.1124/jpet.108.147280.

ABBREVIATIONS: IGF-I, insulin-like growth factor-I; GH, growth hormone; VEGF, vascular endothelial growth factor; CGRP, calcitonin gene-related peptide; TRPV1, transient receptor potential vanilloid 1; WT, wild type; CPZ, capsazepine; BrdU, 5-bromo-2′-deoxyuridine; PKA, protein kinase A; PCR, polymerase chain reaction; DRG, dorsal root ganglion; PBS, phosphate-buffered saline; GFAP, glial fibrillary acidic protein; NTS, solitary tract nucleus; DG, dentate gyrus; PBN, parabrachial nuclei; KT5720, (9*S*,10*S*,12*R*)-2,3,9,10,12-hexahydro-10-hydroxy-9-methyl-1-oxo-9,12-epoxy-1*H*-diindolo[1,2,3-fg:3′,2′,1′-kl]pyrrolo[3,4-i][1,6]-benzo-diazocine-10-carboxylic acid hexyl ester; CT, calcitonin.

The angiogenesis factor vascular endothelial growth factor (VEGF) has an important role in the coupling between angiogenesis and neurogenesis in the brain (Greenberg and Jin, 2005). IGF-I promotes angiogenesis via a VEGF-dependent mechanism in the brain (Lopez-Lopez et al., 2004). IGF-I may promote hippocampal neurogenesis by promoting angiogenesis because vascular elements are thought to be an essential feature of the stem-cell niche in the hippocampus (Palmer et al., 2000).

Capsaicin-sensitive sensory neurons are nociceptive neurons found in many tissues: within the lining epithelia, around blood vessels, and in the nonvascular smooth muscle and myocardium of the atria (Okajima and Harada, 2006). These sensory neurons release calcitonin gene-related peptide (CGRP) after stimulation with a wide variety of noxious physical and chemical stimuli via activation of the transient receptor potential vanilloid 1 (TRPV1) expressed on them (Okajima and Harada, 2006), thereby exerting sensory-efferent functions. CGRP, a 37-amino acid neuropeptide, is produced by alternative splicing of the calcitonin (CT) gene (Okajima and Harada, 2006). It is widely distributed in the central and peripheral nervous systems and has been considered to possess diverse functions (Okajima and Harada, 2006). We reported that CGRP rapidly increases IGF-I production via increasing its transcription in various tissues including the brain of mice administered capsaicin (Harada et al., 2007).

The hippocampus has been shown to receive sensory input from the parabrachial nuclei, the site of termination of the spinothalamic tracts (Suzuki et al., 2002). Nonprincipal neurons in the mouse hippocampus have been shown to be immunoreactive for CGRP (Sakurai and Kosaka, 2007). CGRP receptors are expressed in astrocytes, and CGRP increases intracellular cAMP levels in these cells (Moreno et al., 2002). Because IGF-I is synthesized in astrocytes in the hippocampus (Ye et al., 2004) and cAMP has an important role in the CGRP-induced increase in IGF-I production (Vignery and McCarthy, 1996), stimulation of sensory neurons may increase IGF-I production in astrocytes via increasing CGRP levels in the mouse hippocampus.

Serum levels of IGF-I have been shown to be reduced in patients with Alzheimer's disease, and a significant positive correlation has been shown to exist between serum IGF-I levels and Mini Mental State Examination scores in all of the subjects (Tei et al., 2008). Down-regulation of the IGF-I axis in elderly males is significantly reversed by donepezil (Obermayr et al., 2005).

Based on these observations, donepezil may have a stimulatory effect on sensory neurons in addition to an inhibitory effect on acetylcholinesterase, thereby promoting angiogenesis and neurogenesis through an increase in IGF-I production in the hippocampus. To examine this possibility, we analyzed the effects of two selective acetylcholinesterase inhibitors (donepezil and tacrine) on hippocampal IGF-I production and cognitive function in wild-type (WT) mice, CGRP-knockout [CGRP(−/−)] mice, and WT mice with functional sensory denervation caused by neonatal administration of capsaicin.

Materials and Methods

Reagents. Donepezil hydrochloride [(±)-2-[(1-benzylpiperidin-4-yl)methyl]-5,6-dimethoxy-indan-1-one monohydrochloride] was kindly supplied by Eisai Co. Ltd. (Tokyo, Japan) (Fig. 1) (Sugimoto et al., 2002). Tacrine (9-amino-1,2,3,4-tetrahydroacridine hydrochloride) (Fig. 1) (Sugimoto et al., 2002), capsazepine (CPZ), an inhibitor of TRPV1 activation (Okajima and Harada, 2006), capsaicin, and 5-bromo-2′-deoxyuridine (BrdU) were purchased from Sigma-Aldrich (St. Louis, MO). KT5720, an inhibitor of protein kinase A (PKA), was purchased from Alexis Corporation (Basel, Switzerland). Rat αCGRP was purchased from Peptide Institute Inc. (Osaka, Japan). Human recombinant IGF-I was kindly supplied by Astellas Pharma Inc. (Tokyo, Japan). All other reagents were of analytical grade.

Generation of αCGRP-Deficient Mice. The generation of αCGRP-deficient [CGRP(−/−)] mice was described previously (Oh-hashi et al., 2001). The mouse CT/αCGRP genomic DNA was cloned from a BALB/c mouse genomic library in EMBL3 using synthetic oligonucleotide probes derived from the mouse CT/αCGRP cDNA sequence. A 7.0-kilobase fragment containing exons 3 to 5 of the mouse CT/αCGRP gene was subcloned into pBluescript phagemid (Stratagene, La Jolla, CA). A targeting vector was constructed by replacing the 1.6-kilobase XbaI-XbaI fragment encompassing exon 5, which is specific for αCGRP, with the neomycin resistance gene and flanking the thymidine kinase gene. This plasmid was linearized with NotI and introduced into 129/Sv-derived SM-1 embryonic stem cells by electroporation, after which the cells were selected in medium containing G418 (300 μg/ml) and ganciclovir (2 μM). Homologous recombinants were identified by PCR and Southern blot analysis. Targeted embryonic stem cell clones were injected into C57BL/6 mouse blastocysts to generate chimeric mice. Male chimeras were then cross-bred with C57BL/6 females, and germline transmission was achieved. Littermates obtained by breeding heterozygotes with the genetic background of the 129/SvXC57BL/6 hybrid were used for phenotypic analysis. Only males were used in this study.

Genotype Determination of CGRP(−/−) Pups. Genomic DNA was extracted from tails of mice as described previously (Oh-hashi et al., 2001) and was used for PCR analysis. PCR was performed using the external primers of the replaced gene fragment. The wild-type allele and the mutant allele gave different band sizes. Primer sequences and PCR conditions have been described previously (Oh-hashi et al., 2001).

Isolation and Culture of DRG Neurons. DRG neurons from the lumber, cervical, and thoracic region were dissected from wild-type mice as described previously (Harada et al., 2006). In brief, DRG was placed in ice-cold sterile calcium- and magnesium-free Dulbecco's phosphate-buffered saline (PBS) (Invitrogen, Carlsbad, CA). Ganglia were chopped and incubated at 37°C for 15 min in Dulbecco's PBS containing 20 U/ml papain (Worthington Biochemical Corporation, Lakewood, NJ). The tissue was than incubated at 37°C for 15 min in Dulbecco's PBS containing 4 mg/ml collagenase type II (Worthington Biochemical Corporation). The tissue was incubated for an additional 30 min in Dulbecco's PBS containing 2000 U/ml

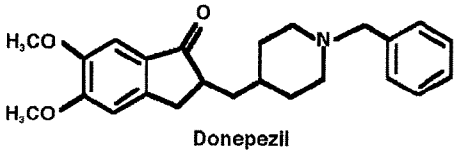

Donepezil

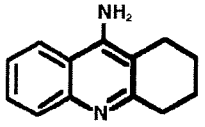

Tacrine

Fig. 1. Structural formulas of donepezil and tacrine.

dispase I (Godo Shusei, Tokyo, Japan) at 37°C. Individual cells were then dissociated by trituration through a fire-polished Pasture pipette. After centrifugation at 250 g for 5 min, the resultant pellet was washed twice in serum-free Ham's F-12 medium (HyClone Laboratories, Logan, UT). Cells were plated on 60-mm polystyrene dish precoated with Vitrogen collagen (Cohesion Technologies, Inc., Palo Alto, CA) in Ham's F-12 medium containing 10% supplemented calf serum, 2 mM glutamine, and 50 ng/ml mouse 2.5S nerve growth factor (Millipore, Billerica, MA). After 24 h, the culture medium was removed and replaced every 2 days.

Release of CGRP from DRG Neurons in Culture and cAMP Measurement. After 5 days in culture, the medium was aspirated gently and washed with serum free Ham's F-12 medium. Cells were incubated with donepezil (1–100 μM), tacrine (1–100 μM), or vehicle for 30 min in Ham's F-12 medium containing 1% supplemented calf serum without nerve growth factor. After incubation, supernatants were sampled and stored at −20°C for CGRP measurement. To determine whether donepezil increased CGRP release from DRG neurons via TRPV1 activation, we examined the effect of CPZ, an inhibitor of TRPV1 activation (Okajima and Harada, 2006), on donepezil-induced CGRP release from DRG neurons. CGRP levels were determined using a specific enzyme immunoassay kit (SPI-BIO, Massy Cedex, France). Recent studies demonstrated that cAMP plays a critical role in CGRP release from sensory neurons by phosphorylating TRPV1 through activation of PKA (Okajima and Harada, 2006), and cAMP-dependent PKA activation is critically involved in CGRP production in DRG neurons (Okajima and Harada, 2006). Therefore, we measured the intracellular cAMP levels in DRG neurons. We examined the effect of KT5720 on CGRP release from DRG neurons at a concentration of 10 μM, as described previously (Harada et al., 2006). After collection of supernatants, plates were placed on ice, media were removed, and cells were washed by ice-cold PBS. Thereafter, ice-cold 65% ethanol was added to each well and placed on ice. Ethanol was collected and dried under nitrogen gas. Intracellular levels of cAMP were determined with an enzyme immunoassay kit (GE Healthcare, Little Chalfont, Buckinghamshire, UK) according to the manufacturer's instructions.

Animal Model. Age-matched (10–12 weeks old, 21–24 g) male C57BL/6 wild-type (Nihon SLC, Hamamatsu, Japan) and CGRP(−/−) mice were used in each experiment. They were maintained under standard conditions of temperature (23–25°C) and on a 12-h light/dark cycle. Food and water were provided ad libitum. The care and handling of the animals were in accordance with the National Institute of Health guidelines. All of the experimental procedures described below were approved by the Nagoya City University Animal Care and Use Committee. The animals were sacrificed at the end of each treatment period. Mice were anesthetized with intraperitoneally injection of ketamine (100 mg/kg) and xylazine (10 mg/kg). separate sets of animals were used for each measurement in the present study.

Administration and Preparation of Various Agents. Capsaicin was dissolved in 10% Tween 80/10% ethanol (10%) and diluted with normal saline. KT5720 and CPZ were dissolved in 10% Tween 20/10% methanol (10%) with normal saline. Donepezil or tacrine was added to the food powder up to final dosage of 1.5 mg/kg per day. Mice were allowed free access to normal food or drug-added food for 4 weeks. CGRP was dissolved in sterile distilled water and injected intraperitoneally 30 min before the behavioral test at a dosage of 10 μg/kg. IGF-I was dissolved in sterile distilled water and injected subcutaneously 30 min before the behavioral test at a dosage of 0.5 mg/kg. Solutions were prepared immediately just before the experiments.

Sensory Denervation by Neonatal Capsaicin Treatment in the WT Mice. Sensory denervation by neonatal capsaicin administration was performed according to a previously described method (Buck and Burks, 1986). Neonatal male WT mouse pups (C57BL/6; Nihon SLC) were weighted and injected subcutaneously into the back with 50 mg/kg capsaicin on postnatal day 2. When these mice reached 10 to 12 weeks of age, they were tested for sensory denervation by applying 0.1 mg/ml capsaicin in saline to the eyes; absence of blinking or scratching confirmed sensory denervation. Capsaicin-treated mice that showed any blinking or scratching were excluded from the study.

Determination of Hippocampus Tissue Levels of CGRP. Tissue levels of CGRP were determined in animals by modification of the methods described previously (Harada et al., 2006). The tissues were weighed and then homogenized in a Polytron-type homogenizer (2 times of 15 s) using 1 ml of 2 N acetic acid. The homogenates were bathed in 90°C water for 20 min and then centrifuged at 4500*g* for 10 min (4°C). CGRP was extracted from the supernatant by using reversed-phase C18 columns (GE Healthcare). Columns were prepared by washing with 5 ml of methanol, followed by 10 ml of water before use. The samples were applied onto the column, followed by washing with 20 ml of 0.1% trifluoroacetic acid. CGRP was eluted with 3 ml of 60% acetonitrile in 0.1% trifluoroacetic acid, and the solvent was evaporated under a stream of nitrogen gas. The concentration of CGRP was assayed by using a specific enzyme immunoassay kit (SPI-BIO). The antiserum cross-reacts 100% with rodent α- and β-CGRP according to the manufacturer's data sheet. Results are expressed as micrograms of CGRP per gram of tissue.

Determination of Hippocampus IGF-I Level. Tissue levels of IGF-I were determined in animals by modification of the methods as described previously (Harada et al., 2007). The hippocampus was minced and homogenized in a Polytron-type homogenizer (2 times of 15 s) using 1 ml of 1 N acetic acid according to the manufacturer's instruction. The homogenates was then centrifuged at 4500*g* for 10 min. The supernatants were kept in a deep freezer at −80°C. The concentration of IGF-I was assayed by using a specific enzyme immunoassay kit (Diagnostic Systems Laboratories Inc., Webster, TX).

Quantitative mRNA Analysis. Quantitative mRNA analysis was performed as described previously (Harada et al., 2007). The tissue was weighed and immersed in liquid nitrogen. Total RNA was extracted from the hippocampus with TRIzol reagent (Invitrogen) according to the manufacturer's instruction. RNA extracted was used as a template for cDNA reverse transcription. Sample cDNAs were amplified in the model 7700 Sequence detector (Applied Biosystems, Foster City, CA) with primers, dual-labeled fluogenic probes, and a Taqman PCR Reagent Kit (Applied Biosystems). Thermal cycler conditions were 10 min at 95°C for deactivation preceding 40 cycles for 15 s at 95°C for denaturation and 1 min at 60°C for bath annealing and extension. Known concentrations of serially diluted IGF-I and β-actin cDNA generated by PCR were used as standards for quantitation of sample cDNA. Copy numbers of cDNA for IGF-I were standardized by those for β-actin from same sample.

Immunohistochemical Staining of IGF-I and Glial Fibrillary Acidic Protein in Hippocampi. The double labeling of immunofluorescent technique was used for immunohistochemical staining of various tissues with anti-IGF-I antibody (Harada et al., 2007). Mice were perfused with 4% paraformaldehyde in phosphate buffer. Tissue blocks were immersed in the same perfusate at 4°C overnight and stored thereafter in a 20% sucrose solution. The tissue blocks of mouse brain were frozen in dry ice-cooled optimal cutting temperature compound (Tissue Tec; Bayer Corp., Emeryville, CA). Frozen coronal sections (18 μm thick) obtained by use of the freezing microtome were stored at −80°C before immunofluorescence. Sections were rinsed in PBS and then incubated for 1 h with PBS, 0.2% Triton X-100, and 0.5% blocking reagent (Roche Diagnostics, Basel, Switzerland) at room temperature. They were incubated overnight at 4°C with mouse anti-IGF-I monoclonal antibody (1:200; Millipore) and rabbit anti-glial fibrillary acidic protein (GFAP) polyclonal antibody (1:1000; Dako Denmark A/S, Glostrup, Denmark). The sections were treated with secondary antibodies Alexa Fluor 568 anti-rabbit IgG for GFAP and Alexa Fluor 488 anti-mouse IgG for IGF-I (1:500; Invitrogen) for 1 h at room temperature. The number of both IGF-I- and GFAP-positive cells was counted in the granule cell layer and in the hilus. The number of cells was counted using one 18 μm-thick section per animals.

c-*fos* Immunohistochemistry. Immunohistochemical staining of c-*fos* in mice brain was performed according to the method as described previously (Linden et al., 2004). Mice were anesthetized (5% isoflurane) and decapitated. Brains were rapidly removed and frozen in dry ice-cooled optimal cutting temperature compound (Tissue Tec; Bayer Corp). Frozen coronal sections (18 μm thick) obtained by use of the freezing microtome were stored at −80°C before immunofluorescence. Slides were removed from the freezer, allowed to air-dry for 15 min, and fixed for 10 min in ice-cold 4% paraformaldehyde in PBS (pH 7.4). Sections were rinsed in PBS and then incubated for 1 h with PBS, 0.2% Triton X-100, and 0.5% blocking reagent (Roche Diagnostics) at room temperature. They were incubated overnight at 4°C with rabbit anti-c-*fos* polyclonal antibody (1:500; Santa Cruz Biotechnology Inc., Santa Cruz, CA). The sections were treated with secondary antibody Alexa Fluor 568 anti-rabbit IgG (1:500; Invitrogen) for 1 h at room temperature. After staining, samples were examined under a fluorescence microscope (Axio Imager A1; Carl Zeiss GmbH, Jena, Germany).

Double Stain Immunohistochemistry for CD31, GFAP, or Calbindin-D28k with BrdU. We used BrdU labeling to monitor proliferation and double immunofluorescent labeling for BrdU and cell-specific markers to determine the phenotype of the progenitor progeny. During the last 5 days of each treatment period, the animals for determination of BrdU-labeled nuclei received a daily intraperitoneal injection of BrdU at a dosage of 50 mg/kg. Angiogenesis and neurogenesis in the mouse brains was monitored by BrdU incorporation into the nuclei of dividing cells as described previously (Aberg et al., 2000). Samples were treated for DNA denaturation in the following manner: tissues were incubated in 50% formamide in 2× SSC buffer (1× SSC, 0.3 M NaCl, and 0.03 M sodium citrate) at 65°C for 2 h, rinsed in PBS, and then incubated for 30 min with 2 N HCl at 37°C. They were rinsed for 10 min at room temperature in 0.1 M boric acid (pH 8.4). The tissue was rinsed with PBS three times followed by incubation in PBS containing 0.2% Triton X-100, and 0.5% blocking reagent (Roche Diagnostics) for 1 h and then with primary rat anti-CD31 monoclonal antibody (1:200; BD Biosciences Pharmingen, San Diego, CA), with mouse anti-BrdU monoclonal antibody (1:100; Invitrogen) or rabbit anti-GFAP polyclonal antibody (1:1000; Dako Denmark A/S) or mouse anti-calbindin-D28k monoclonal antibody (1:200; Abcam, Inc., Cambridge, UK), or with rat anti-BrdU monoclonal antibody (1:400; Abcam, Inc.) overnight at 4°C. The sections were treated with secondary antibodies Alexa Fluor 594 anti-rat IgG for CD31, Alexa Fluor 488 anti-mouse IgG for BrdU (anti-mouse), Alexa Fluor 568 anti-rabbit IgG for GFAP, Alexa Fluor 488 anti-mouse IgG for calbindin-D28k, and Alexa Fluor 594 anti-rat IgG for BrdU (anti-rat) (1:500; Invitrogen) for 1 h at room temperature. After staining samples were examined under a fluorescence microscope (Axio Imager A1; Carl Zeiss GmbH), BrdU-positive cells were counted in the granule cell layer and in the hilus. The number of cells was counted using one 18 μm-thick section per animal.

Morris Water Maze Task. Behavioral testing was conducted as described previously (Ryan et al., 2008). We used a circular pool (150 cm diameter). The pool was filled with water at 30°C and contained a round-shaped transparent acrylic platform (10 cm diameter). In the task, the platform was submerged 1 cm below the surface of the water and located in the southeast quadrant of the pool throughout the trials. After a mouse was put into the pool, each had a maximum of 90 s to locate and climb onto the platform (one trial). When a mouse located the platform, it was allowed to stay on it for 20 s. The mouse that did not find the platform in the allowed time was placed on it by the experimenter and left there for 20 s. Latency to reach the platform was monitored. Each mouse was subjected to one trial per day. The task consisted of 5 days of trials. Two hours after the last trial, the probe test was carried out. For this test, the platform was removed from the pool, and the trial was performed with the cutoff time of 90 s. The time spent in the target area (zone radius: 30 cm, three times the target diameter) was recorded as a percentage of the trial time in the pool.

Statistical Analysis. Data are expressed as the mean ± S.D. The results were compared using an analysis of variance followed by Scheffé's post hoc test. A level of $p < 0.05$ was considered statistically significant.

Results

Effects of Donepezil and Tacrine on CGRP Release and Cellular cAMP Levels in DRG Neurons Isolated from WT Mice. Donepezil at concentrations of 1, 10, and 100 μM increased the release of CGRP from DRG neurons isolated from WT mice (Fig. 2A). Tacrine did not increase the CGRP release from DRG neurons (Fig. 2A). Cyclic AMP has been shown to play an important role in the release of CGRP from sensory neurons upon activation (Okajima and Harada, 2006). Donepezil at concentrations of >1 μM increased cellular cAMP levels in DRG neurons, whereas tacrine did not (Fig. 2B). Pretreatment with CPZ reversed the donepezil-induced increase in CGRP release from DRG neurons (Fig. 3). TRPV1 is activated by phosphorylation through cAMP-dependent PKA (Okajima and Harada, 2006). Donepezil may increase CGRP release from DRG neurons by activating PKA because donepezil was found to increase cellular cAMP levels in DRG neurons. To examine this possibility, we analyzed the effect of pretreatment with the PKA inhibitor KT5720 on donepezil-induced CGRP release from DRG neurons isolated from WT mice. Donepezil-induced increase in CGRP release

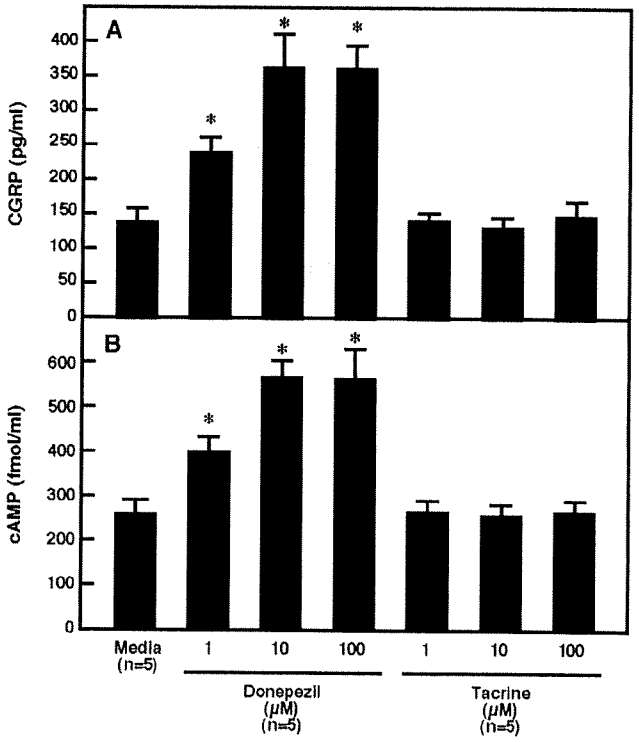

Fig. 2. Effects of donepezil and tacrine on CGRP release from DRG neurons (A) and intracellular cAMP levels (B) in DRG neurons isolated from WT mice. DRG neurons were incubated with donepezil (1–100 μM) or tacrine (1–100 μM) for 30 min. Supernatants were sampled, and CGRP levels were measured by enzyme immunoassay. Intracellular cAMP levels were measured by enzyme immunoassay. Each value represents the mean ± S.D. derived from five experiments. *, $p < 0.01$ versus media.

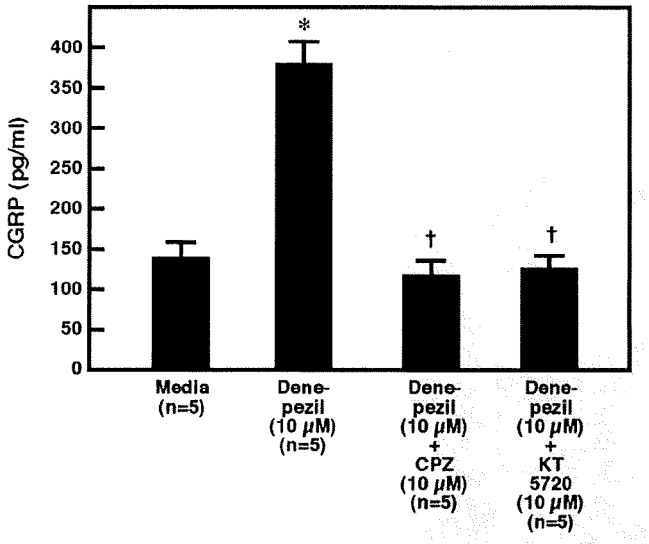

Fig. 3. Effects of CPZ and KT5720 on donepezil-induced increase in CGRP release from DRG neurons isolated from WT mice. DRG neurons were incubated with donepezil (10 μM) for 30 min in the presence or absence of the inhibitor of TRPV1 activation CPZ (10 μM) or the PKA inhibitor KT5720 (10 μM). Each value represents the mean ± S.D. from five experiments. *, $p < 0.01$ versus media; †, $p < 0.01$ versus donepezil.

from DRG neurons was completely reversed by pretreatment with KT5720 (Fig. 3).

Effects of Donepezil and Tacrine on Tissue Levels of CGRP, IGF-I, and IGF-I mRNA in the Hippocampus of WT Mice, CGRP(−/−) Mice, and WT Mice Subjected to Functional Denervation. To examine whether donepezil increases tissue levels of CGRP, IGF-I, and IGF-I mRNA in the hippocampus through sensory neuron stimulation in mice, we determined tissue levels of these substances in the hippocampus after oral administration of donepezil for 4 weeks in WT mice, CGRP(−/−) mice, and WT mice subjected to functional denervation. At baseline, tissue levels of CGRP, IGF-I, and IGF-I mRNA in the hippocampus of WT mice were significantly higher than those in the hippocampus of CGRP(−/−) mice and WT mice subjected to functional denervation ($p < 0.01$) (Fig. 4). Administration of donepezil significantly increased hippocampal tissue levels of CGRP, IGF-I, and IGF-I mRNA in WT mice ($p < 0.01$), whereas such increases were not observed in the hippocampus of CGRP(−/−) mice and WT mice subjected to functional denervation (Fig. 4). Increase in the levels of CGRP, IGF-I, and IGF-I mRNA was not observed in WT mice after tacrine administration for 4 weeks (Fig. 4).

Effects of Donepezil and Tacrine on Immunohistochemical Expression of IGF-I in the Hippocampus of WT Mice, CGRP(−/−) Mice, and WT Mice Subjected to Functional Denervation. Increase in the immunohistochemical expression of IGF-I in the dentate gyrus (DG) was observed after 4 weeks of donepezil administration in WT mice. IGF-I immunoreactivity was colocalized with immunoreactivity for the astrocyte marker GFAP in WT mice (Figs. 5, A—C, and 6), and increase in the IGF-I immunoreactivity colocalized with GFAP immunoreactivity was observed after donepezil administration in WT mice (Figs. 5, D—F, and 6). Such an increase in IGF-I expression was not observed in WT mice after tacrine administration for 4 weeks (Figs. 5, G—I,

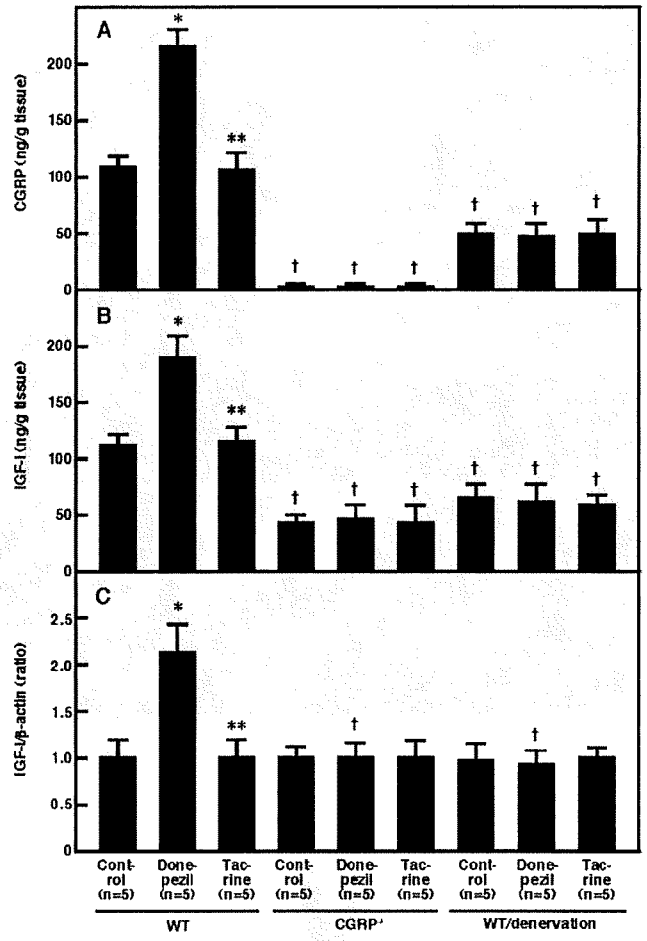

Fig. 4. Effects of donepezil and tacrine on hippocampal levels of CGRP (A), IGF-I (B), and IGF-I mRNA (C) in WT mice, CGRP(−/−) mice, and WT mice subjected to functional denervation (WT/denervation). All tissues were removed at 4 weeks after oral administration of donepezil (1.5 mg/kg/day), tacrine (1.5 mg/kg/day), or vehicle. Values are means ± S.D. derived experiments using five animals. *, $p < 0.01$ versus vehicle; **, $p < 0.01$ versus donepezil; †, $p < 0.01$ versus WT.

and 6). An increase of IGF-I expression was not observed in DG after donepezil administration in CGRP(−/−) mice and the WT mice subjected to functional denervation (data not shown).

Effect of Donepezil on c-*fos* Expression in the Spinal and Supraspinal Nervous Tissues of WT Mice, CGRP(−/−) Mice, and WT Mice Subjected to Functional Denervation. To analyze the mechanism and pathway of the relay system that leads to the increase in hippocampal IGF-I production in WT mice administered donepezil, we determined c-*fos* expression in the spinal and supraspinal nervous tissues of WT mice, CGRP(−/−) mice, and WT mice subjected to functional denervation after 4 weeks of oral administration of donepezil. In WT mice, increase in c-*fos* expression was observed in the dorsal horns (laminae I–II) of the spinal cord and, supraspinally, in the solitary tract nucleus (NTS), parabrachial nuclei (PBN), and the hippocampus (Figs. 7 and 8); no such increase in c-*fos* expression was noted in WT mice after administration of tacrine for 4 weeks (Fig. 8). An increase in c-*fos* expression was not observed in the same tissues after donepezil admin-

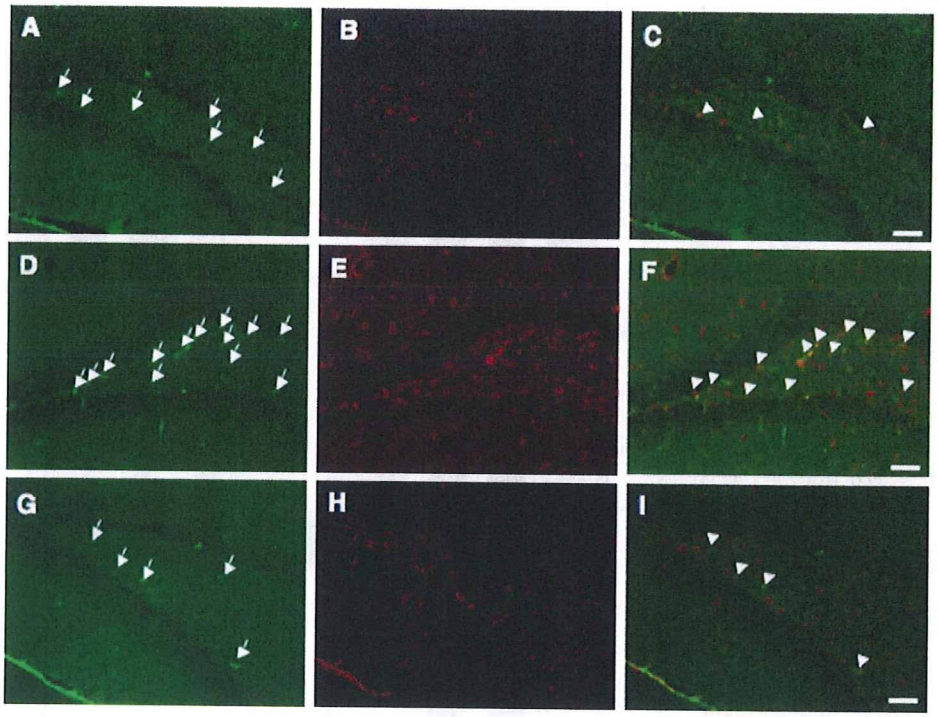

Fig. 5. Effect of donepezil on immunohistochemical expression of IGF-I in the hippocampus of WT mice. Fluorescent photomicrographs of cryostat sections showing IGF-I expression in the hippocampus of WT mice. Double labeling of IGF-I (green) and GFAP (red) showed the localization of IGF-I in the hippocampus. Immunohistochemical expression of the dentate gyrus in a vehicle (A, B, and C), a donepezil-treated animal (D, E, and F), and a tacrine-treated animal (G, H, and I) is shown in the insets. Five animals in each group were examined, and typical results are shown. Arrows indicate IGF-I-positive staining. Arrowheads indicate colocalization of IGF-I and GFAP-positive staining. Scale bars = 50 μm.

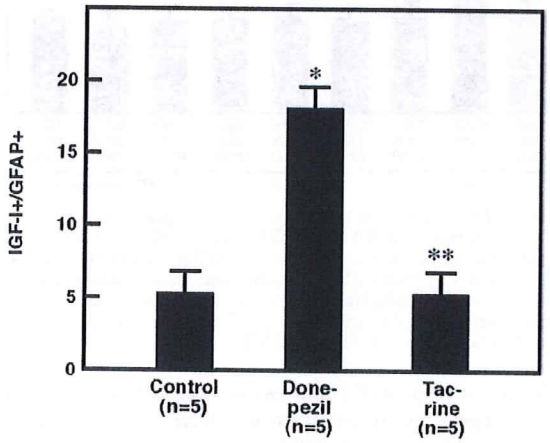

Fig. 6. Effects of donepezil and tacrine on the number of cells showing colocalization of IGF-I- and GFAP-positive staining in the hippocampus of WT mice. Values are means ± S.D. derived from five animal experiments. *, $p < 0.01$ versus vehicle; **, $p < 0.01$ versus donepezil.

istration in CGRP(−/−) mice and WT mice subjected to functional denervation (data not shown).

Effects of Donepezil and Tacrine on Hippocampal Angiogenesis and Neurogenesis in WT Mice, CGRP(−/−) Mice, and WT Mice Subjected to Functional Denervation. The number of BrdU-immunoreactive cells in the DG was significantly higher in WT mice than in CGRP(−/−) mice and WT mice subjected to functional denervation ($p < 0.01$) (Fig. 9A). Further significant increase in the number of BrdU-immunoreactive cells was observed in the DG of WT mice after 4 weeks of administration of donepezil ($p < 0.01$), whereas no such increase was observed in CGRP(−/−) mice and WT mice subjected to functional denervation (Fig. 9A).

Colocalization of BrdU immunoreactivity with immunoreactivity for the vascular endothelial cell marker CD31, the granule cell marker calbindin-D28k, and the astrocyte marker GFAP was examined to determine the phenotype of progenitor cell progeny in the DG after donepezil administration in WT mice, CGRP(−/−) mice, and WT mice subjected to functional denervation (Fig. 9, B–D). Significantly higher numbers of BrdU+/CD31+, BrdU+/calbindin-D28k+, and BrdU+/GFAP+ cells were observed in the DG of WT mice than in those of CGRP(−/−) mice and WT mice subjected to functional denervation ($p < 0.01$) (Fig. 9, B–D). A significant increase in the number of BrdU+/CD31+ and BrdU+/calbindin-D28k+ cells, but not BrdU+/GFAP+ cells, in the DG was observed after 4 weeks of administration of donepezil in WT mice, whereas no such increase in the number of BrdU+/CD31+ and BrdU+/calbindin-D28k+ cells was noted in WT mice administered tacrine for 4 weeks (Fig. 9, B–D). No increase in the number of any of these cells in the DG was observed after donepezil administration in CGRP(−/−) mice and WT mice subjected to functional denervation (Fig. 9, B–D).

Effects of Donepezil and Tacrine on the Spatial Learning Function in WT Mice, CGRP(−/−) Mice, and WT Mice Subjected to Functional Denervation. To determine whether donepezil improves the cognitive function in mice by stimulating sensory neurons, we examined the effect of donepezil administration on spatial learning in WT mice, CGRP(−/−) mice, and WT mice subjected to functional denervation using the Morris water maze test for 5 consecutive days. In animals not administered donepezil, a significant improvement in spatial learning on days 3, 4, and 5 compared with that on day 1 was observed in WT mice ($p < 0.01$) (Fig. 10A); no such improvement was noted through the 5 days in CGRP(−/−) mice and WT mice subjected to functional denervation (Fig. 10, B and C). In WT mice, the improvement in spatial learning on days 2, 3, 4, and 5 was

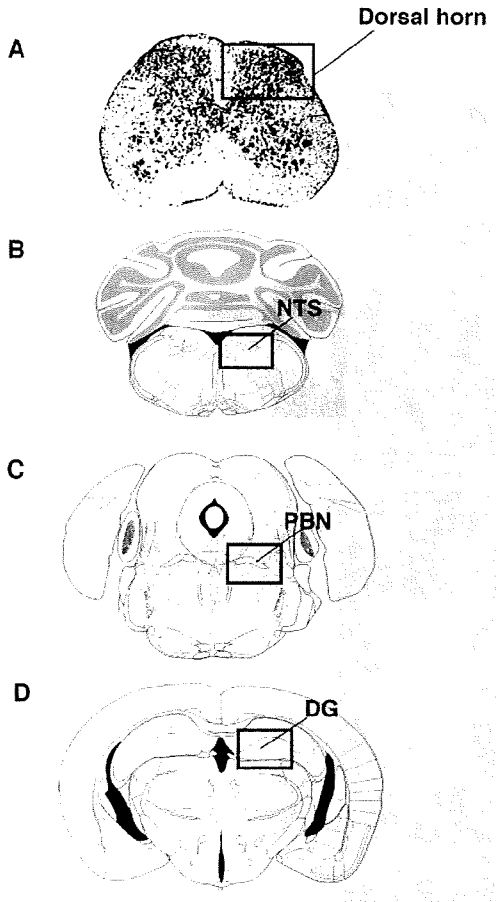

Fig. 7. Schematic diagrams of spinal cord (A) [Reprinted by permission of the publisher from *Atlas of the Mouse Brain and Spinal Cord* by Richard L. Sidman, Jay B. Angevine, and Elizabeth Taber Pierce, p. 261, L2, Cambridge, MA; Harvard University Press, Copyright © 1971 by the President and Fellows of Harvard College] and brain sections (B, C, and D) [adapted from Franklin KBJ and Paxinos G (2008) *The Mouse Brain in Stereotaxic Coordinates*, Academic Press, Inc., San Diego. Copyright © 2008, Elsevier] where select spinal cord and brain regions were analyzed for c-*fos* expression. The location and approximate size of the analyzed area for each region are indicated. A, dorsal horn of spinal cord. B, NTS, solitary tract nucleus. C, PBN. D, DG, granular cell layer of the dentate gyrus.

significantly enhanced in animals treated with donepezil for 4 weeks compared with that in those not administered donepezil (Fig. 10A). Donepezil did not improve spatial learning through the 5 days in CGRP(−/−) mice and WT mice subjected to functional denervation (Fig. 10, B and C). Tacrine did not improve spatial learning in the WT mice (Fig. 10A). Administration of CGRP and IGF-I significantly improved spatial learning on days 3, 4, and 5 in CGRP(−/−) mice and WT mice subjected to functional denervation compared with that in control animals (Fig. 10, B and C). Similar effects were observed with time spent in the target area (probe test). Donepezil improved the performance in the probe test in WT mice but not in CGRP(−/−) mice and WT mice subjected to functional denervation (Fig. 11). Tacrine did not affect the performance in WT mice (Fig. 11). Administration of CGRP and IGF-I markedly inhibited the deterioration in the performance of CGRP(−/−) mice and WT mice subjected to functional denervation (Fig. 11).

Discussion

In the present study, donepezil increased CGRP release from DRG neurons isolated from WT mice in vitro. Pretreatment with CPZ, an inhibitor of TRPV1 activation, reversed the donepezil-induced increase in the CGRP release from DRG neurons, suggesting that TRPV1 activation may be critically involved in the donepezil-induced increase of CGRP release from sensory neurons. The mechanism(s) by which donepezil activates TRPV1 is still not fully understood. PKA activation has been shown to induce phosphorylation of TRPV1, thereby sensitizing the sensory neurons to activation by endogenous agonists (Okajima and Harada, 2006). Consistent with this hypothesis are observations in the present study demonstrating that donepezil increased cellular cAMP levels in DRG neurons and that the donepezil-induced increase of CGRP release from DRG neurons was completely inhibited by the PKA inhibitor KT5720. These observations suggest that donepezil may increase the release of CGRP from sensory neurons by activating PKA through an increase in cellular cAMP levels in sensory neurons.

The hippocampal tissue levels of IGF-I and IGF-I mRNA were significantly lower in CGRP(−/−) mice and WT mice subjected to functional denervation than in WT mice. Oral administration of donepezil increased the hippocampal tissue levels of CGRP, IGF-I, and IGF-I mRNA and the immunohistochemical expression of IGF-I in WT mice, but not in the CGRP(−/−) mice and WT mice subjected to functional denervation. These observations strongly suggest that donepezil administration may induce the transcription and production of IGF-I in the hippocampus by increasing hippocampal CGRP levels. Consistent with this notion is our previous report demonstrating that stimulation of sensory neurons by capsaicin administration induced transcription and production of IGF-I in various tissues by increasing CGRP levels (Harada et al., 2007).

IGF-I immunoreactivity was colocalized with immunoreactivity for the astrocyte marker GFAP in the DG of WT mice administered donepezil. This observation is consistent with reports showing that astrocytes can produce IGF-I in the hippocampus (Ye et al., 2004). CGRP has been shown to increase cAMP levels via CGRP receptor activation in astrocytes (Lazar et al., 1991). Because cAMP plays an important role in IGF-I production (Vignery and McCarthy, 1996), stimulation of sensory neurons by donepezil may increase CGRP levels in the hippocampus, thereby increasing IGF-I production via inducing an increase in cAMP levels in astrocytes. Precisely which cells produce CGRP in the hippocampus of WT mice administered donepezil is presently unknown.

To examine the mechanism(s) by which afferent sensory information arising from stimulation by donepezil is transmitted to the hippocampus, we analyzed c-*fos* expression in spinal and supraspinal nervous tissues in WT mice, CGRP(−/−) mice, and WT mice subjected to functional denervation after 4 weeks of administration of donepezil. In WT mice, increase in c-*fos* expression was observed in the dorsal horns (laminae I–II) of the spinal cord and, supraspinally, in the NTS, PBN, and hippocampus after donepezil administration. These observations strongly suggest that nociceptive information arising from stimulation with donepezil in the gastrointestinal tract may be transmitted via the spinopara-

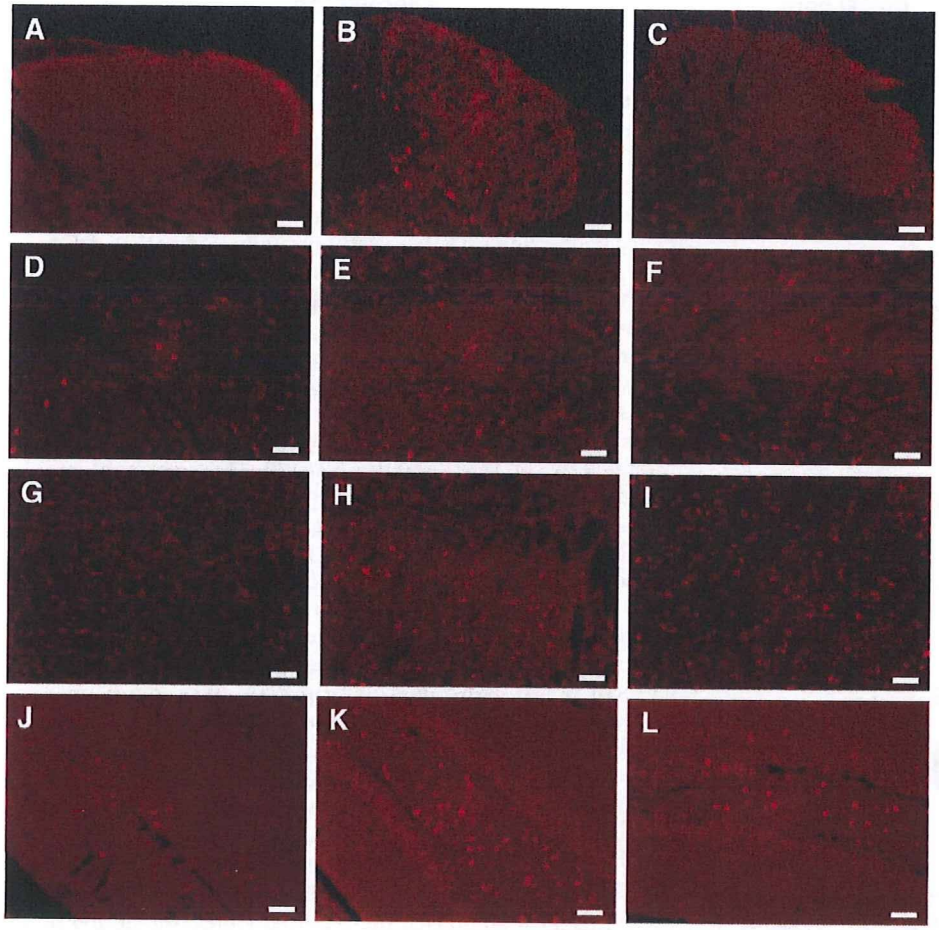

Fig. 8. Effect of donepezil on c-*fos* expression in spinal and supraspinal tissue levels in WT mice. All tissues were removed 4 weeks after oral administration of donepezil (1.5 mg/kg/day) (B, E, H, and K), tacrine (1.5 mg/kg/day) (C, F, I, and L), and vehicle (A, D, G, and J). Immunohistochemical expression of c-*fos* in the dorsal horn of the spinal cord is indicated in Fig. 6A (A–C), solitary tract nucleus is indicated in Fig. 6B (D–F), medial parabrachial nucleus is indicated in Fig. 6C (G–I), and granular cell layer of the dentate gyrus is indicated in Fig. 6D (J–L). Five animals in each group were examined, and typical results are shown. Scale bars = 50 μm.

brachial circuits, including NTS as a relay point (Castle et al., 2005).

Nonprincipal neurons have been shown to be immunoreactive for CGRP in the mouse hippocampus (Sakurai and Kosaka, 2007). Hippocampal nonprincipal neurons are innervated by GABAergic neurons projecting from the medial septum (Gulyas et al., 1991). Because the medial septum receives sensory input from PBN where the spinothalamic tracts terminate (Castle et al., 2005), the increase in hippocampal tissue CGRP levels in WT mice administered donepezil may be a consequence of activation of the hippocampal nonprincipal neurons by GABAergic neurons projecting into them from the medial septum. These observations suggest that CGRP released from the hippocampal nonprincipal neurons acts on astrocytes via CGRP receptors, thereby increasing IGF-I production in the hippocampus of WT mice administered donepezil.

In contrast with observations in WT mice administered donepezil, induction of c-*fos* expression was not observed in the spinal or supraspinal nervous tissues of CGRP(−/−) mice and WT mice subjected to functional denervation after donepezil administration. These observations suggest that donepezil may stimulate sensory neurons in the gastrointestinal tract, thereby increasing hippocampal IGF-I production, and that CGRP may function as a transmitter in the pathway involved in this sensory nervous relay system. Consistent with this hypothesis are reports demonstrating CGRP expression at synaptic contacts between the primary afferent sensory neurons and spinothalamic tract neurons in the dorsal horn of the spinal cord (Carlton et al., 1990), in spinothalamic tract cells, and in nerve fibers originating from the PBN (Tie-Jun et al., 2001).

The number of CD31+, calbindin-D28k+, and GFAP+ cells in the BrdU-immunoreactive cells of the DG in CGRP(−/−) mice and WT mice subjected to functional denervation was significantly lower than the corresponding number in WT mice, suggesting that CGRP and/or IGF-I may be deeply related to neural stem cell proliferation in the mouse hippocampus. Consistent with this hypothesis is a report demonstrating that IGF-I is necessary for angiogenesis in the adult mouse brain (Lopez-Lopez et al., 2004) and for neural stem cell proliferation acting via the mediation of epidermal growth factor and fibroblast growth factor-2 (Arsenijevic et al., 2001).

Donepezil increased the number of BrdU+ cells as well as BrdU+ and calbindin-D28k+ double-positive cells, but not that of BrdU+ and GFAP+ cells, in the DG of WT mice. Tacrine had no such effect on the number of either BrdU+ cells or BrdU+ and calbindin-D28k+ double-positive cells. Donepezil had no effect on the number of these cells in the DG of CGRP(−/−) mice and WT mice subjected to functional denervation. Peripheral infusion of IGF-I was shown to selectively induce angiogenesis via a VEGF-dependent mechanism in the adult mouse brain (Lopez-Lopez et al., 2004) and

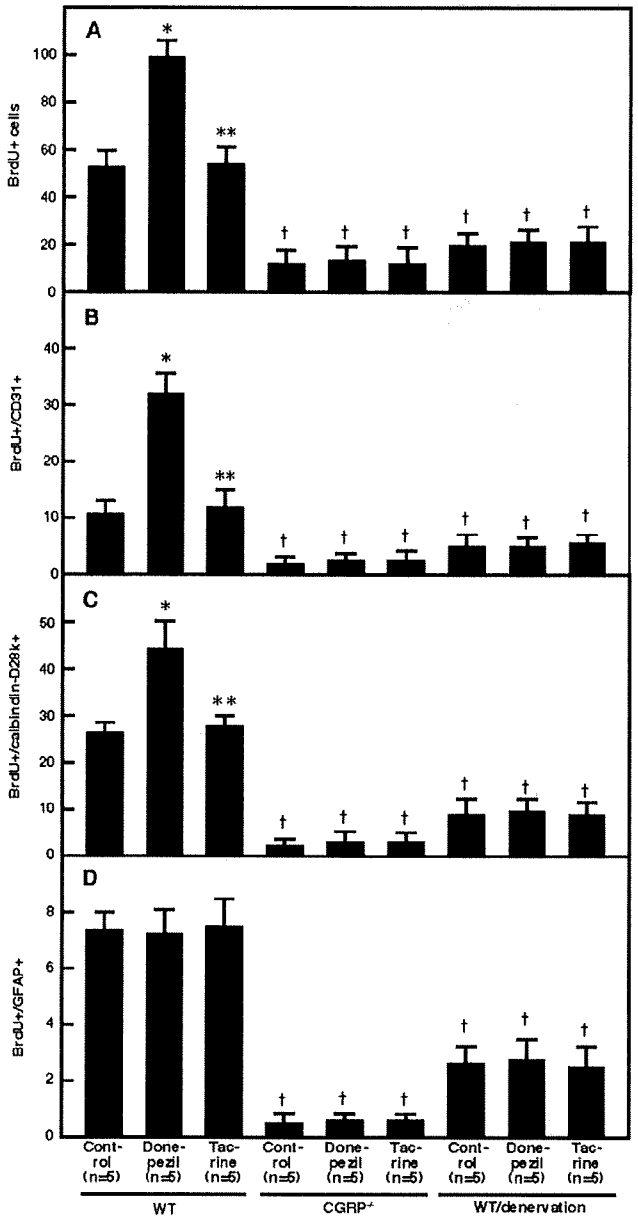

Fig. 9. Effects of donepezil and tacrine on the hippocampal angiogenesis and neurogenesis in WT mice, CGRP(−/−) mice, and WT mice subjected to functional denervation (WT/denervation). Donepezil enhanced neurovascular progenitors in the DG. Angiogenesis was examined by the colocalization of the endothelial marker CD31 and the proliferation marker BrdU. Neurogenesis was examined by the colocalization of the neuronal marker calbindin-D28k and the proliferation marker BrdU. All tissues were removed 5 days after BrdU injections. In each experiment, data were obtained from five separate experiments, with one animal in each treatment condition. Quantitative analysis of the number of BrdU+ (A), BrdU+/CD31+ (B), BrdU+/calbindin-D28k+ (C), and BrdU+/GFAP+ (D) cells in DG were performed. Values are expressed as means ± S.D. derived from five animal experiments. *, $p < 0.01$ versus vehicle; **, $p < 0.01$ versus donepezil; †, $p < 0.01$ versus WT.

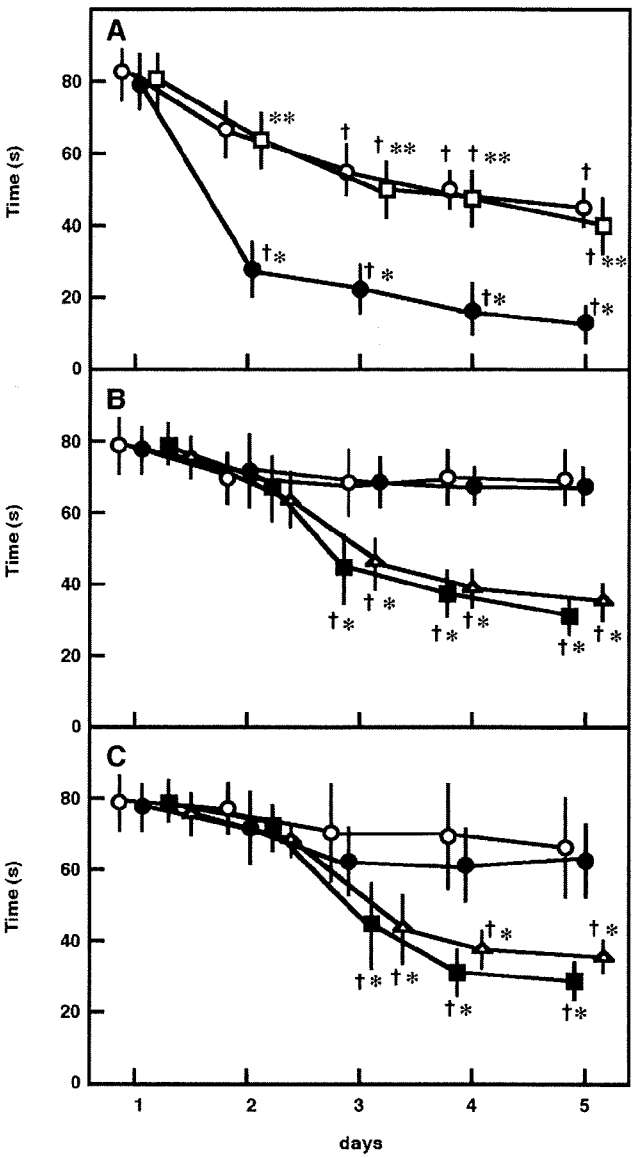

Fig. 10. Effects of donepezil and tacrine on the spatial learning function in WT mice (A), CGRP(−/−) mice (B), and WT mice subjected to functional denervation (C). Each value is expressed as the mean ± S.D. derived from five animal experiments. A, ○, vehicle; ●, donepezil; □, tacrine. B, ○, vehicle; ●, donepezil; ■, CGRP; △, IGF-I. C, ○, vehicle; ●, donepezil; ■, CGRP; △, IGF-I. A, †, $p < 0.01$ versus day 1; *, $p < 0.01$ versus vehicle; **, $p < 0.01$ versus donepezil. B, †, $p < 0.01$ versus day 1; *, $p < 0.01$ versus vehicle. C, †, $p < 0.01$ versus day1; *, $p < 0.01$ versus vehicle.

neurogenesis in the adult rat hippocampus (Aberg et al., 2000). These observations strongly suggest that stimulation of sensory neurons by donepezil may induce angiogenesis and neurogenesis by inducing IGF-I production via an increase in CGRP levels in the mouse hippocampus. Because angiogenesis has been shown to provide a favorable environment for neuronal stem cell proliferation via activation of a VEGF-dependent mechanism (Palmer et al., 2000), the hippocampal neurogenesis induced by donepezil administration in WT mice may be mediated by angiogenesis.

IGF-I exerts beneficial effects against the decline of cognitive function by inducing neurogenesis in the hippocampus (Aberg et al., 2000), suggesting that donepezil may improve the cognitive function by inducing IGF-I production through promoting CGRP release in the mouse hippocampus. Consistent with this hypothesis are observations in the present

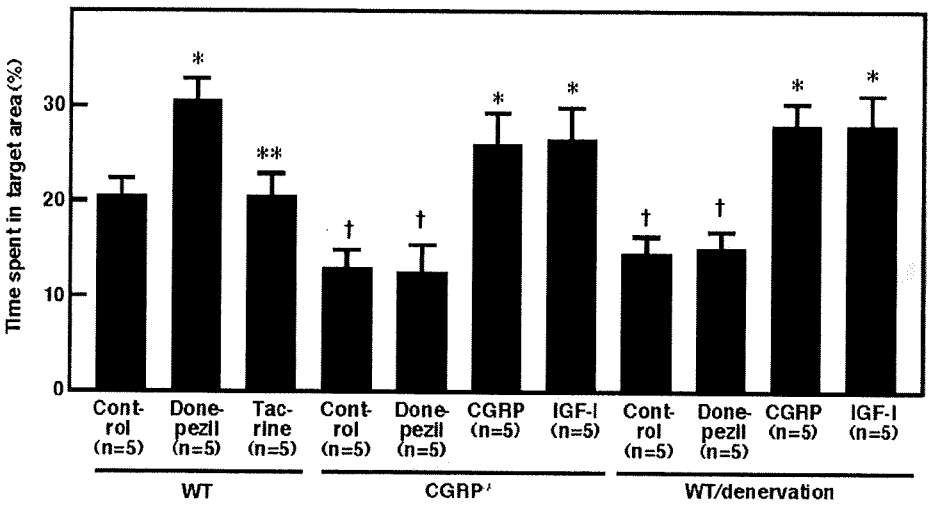

Fig. 11. Effects of donepezil and tacrine on the spatial learning function (probe test) in WT mice, CGRP(−/−) mice, and WT mice subjected to functional denervation (WT/denervation). Each value is expressed as the mean ± S.D. derived from five animal experiments. *, $p < 0.01$ versus control; **, $p < 0.01$ versus donepezil; †, $p < 0.01$ versus WT.

study demonstrating that donepezil significantly improved spatial learning function in WT mice but not in CGRP(−/−) mice and WT mice subjected to functional denervation. These observations suggest that stimulation of sensory neurons with donepezil may increase the release of CGRP, inducing IGF-I production in the mouse hippocampus, thereby improving cognitive function.

Acetylcholine is one of the most important neurotransmitters involved in learning and memory (Kotani et al., 2006). Activation of the central cholinergic function has been considered to enhance hippocampal neurogenesis, thereby contributing to the improvement in cognitive function. In this context, donepezil, a selective acetylcholinesterase inhibitor, ameliorates cognitive impairment in Alzheimer's disease (Winblad et al., 2006). Tacrine, another selective acetylcholinesterase inhibitor, did not stimulate sensory neurons as shown in the present study. Tacrine also was shown to have no effect on hippocampal tissue levels of CGRP, IGF-I, and IGF-I mRNA and spatial learning in WT mice. These observations strongly suggest that stimulation of sensory neurons by donepezil may not be dependent on its acetylcholinesterase-inhibiting activity, but rather on some other unknown pharmacological actions.

Taken together, the observations of the present study strongly suggest that peripheral sensory nerve stimulation with donepezil may increase tissue levels of CGRP in the hippocampus, thereby inducing IGF-I production as well as promoting angiogenesis and neurogenesis to produce improvement in cognitive function in mice.

Of the various regulators of IGF-I production, GH is probably the most important, capable of regulating it via endocrine and paracrine mechanisms (Okajima and Harada, 2008). IGF-I production in the brain is not reduced in GH receptor-knockout mice (Lupu et al., 2001). These observations suggest that hippocampal IGF-I production may be GH-independent and that sensory neurons may be involved at least in part in the GH-independent IGF-I production mechanism(s) in the hippocampus.

Because the serum levels of IGF-I in patients with Alzheimer's disease have been shown to be significantly lower than those in controls without dementia (Watanabe et al., 2005), the observations of the present study indicate that pharmacological stimulation of sensory neurons may be useful for improving cognitive function via promotion of angiogenesis and neurogenesis in the hippocampus through induction of IGF-I production in patients with Alzheimer's disease.

References

Aberg MA, Aberg ND, Hedbäcker H, Oscarsson J, and Eriksson PS (2000) Peripheral infusion of IGF-I selectively induces neurogenesis in the adult rat hippocampus. *J Neurosci* **20**:2896–2903.

Arsenijevic Y, Weiss S, Schneider B, and Aebischer P (2001) Insulin-like growth factor-I is necessary for neural stem cell proliferation and demonstrates distinct actions of epidermal growth factor and fibroblast growth factor-2. *J Neurosci* **21**:7194–7202.

Buck SH and Burks TF (1986) The neuropharmacology of capsaicin: review of some recent observations. *Pharmacol Rev* **38**:179–226.

Carlton SM, Westlund KN, Zhang DX, Sorkin LS, and Willis WD (1990) Calcitonin gene-related peptide containing primary afferent fibers synapse on primate spinothalamic tract cells. *Neurosci Lett* **109**:76–81.

Castle M, Comoli E, and Loewy AD (2005) Autonomic brainstem nuclei are linked to the hippocampus. *Neuroscience* **134**:657–669.

Franklin KBJ and Paxinos G (2008) *The Mouse Brain in Stereotaxic Coordinates*. Academic Press, Inc, San Diego.

Greenberg DA and Jin K (2005) From angiogenesis to neuropathology. *Nature* **438**:954–959.

Gulyás AI, Tóth K, Dános P, and Freund TF (1991) Subpopulations of GABAergic neurons containing parvalbumin, calbindin D28k, and cholecystokinin in the rat hippocampus. *J Comp Neurol* **312**:371–378.

Harada N, Okajima K, Kurihara H, and Nakagata N (2007) Stimulation of sensory neurons by capsaicin increases tissue levels of IGF-I, thereby reducing reperfusion-induced apoptosis in mice. *Neuropharmacology* **52**:1303–1311.

Harada N, Okajima K, Uchiba M, Kurihara H, and Nakagata N (2006) Antithrombin reduces reperfusion-induced liver injury in mice by enhancing sensory neuron activation. *Thromb Haemost* **95**:788–795.

Kotani S, Yamauchi T, Teramoto T, and Ogura H (2006) Pharmacological evidence of cholinergic involvement in adult hippocampal neurogenesis in rats. *Neuroscience* **142**:505–514.

Landi F, Capoluongo E, Russo A, Onder G, Cesari M, Lulli P, Minucci A, Pahor M, Zuppi C, and Bernabei R (2007) Free insulin-like growth factor-I and cognitive function in older persons living in community. *Growth Horm IGF Res* **17**:58–66.

Lazar P, Reddington M, Streit W, Raivich G, and Kreutzberg GW (1991) The action of calcitonin gene-related peptide on astrocyte morphology and cyclic AMP accumulation in astrocyte cultures from neonatal rat brain. *Neurosci Lett* **130**:99–102.

Linden AM, Greene SJ, Bergeron M, and Schoepp DD (2004) Anxiolytic activity of the MGLU2/3 receptor agonist LY354740 on the elevated plus maze is associated with the suppression of stress-induced c-Fos in the hippocampus and increases in c-Fos induction in several other stress-sensitive brain regions. *Neuropsychopharmacology* **29**:502–513.

Lopez-Lopez C, LeRoith D, and Torres-Aleman I (2004) Insulin-like growth factor I is required for vessel remodeling in the adult brain. *Proc Natl Acad Sci U S A* **101**:9833–9838.

Lupu F, Terwilliger JD, Lee K, Segre GV, and Efstratiadis A (2001) Roles of growth hormone and insulin-like growth factor 1 in mouse postnatal growth. *Dev Biol* **229**:141–162.

Moreno MJ, Terrón JA, Stanimirovic DB, Doods H, and Hamel E (2002) Characterization of calcitonin gene-related peptide (CGRP) receptors and their receptor-activity-modifying proteins (RAMPs) in human brain microvascular and astroglial cells in culture. *Neuropharmacology* **42**:270–280.

Obermayr RP, Mayerhofer L, Knechtelsdorfer M, Mersich N, Huber ER, Geyer G, and Tragl KH (2005) The age-related down-regulation of the growth hormone/

insulin-like growth factor-1 axis in the elderly male is reversed considerably by donepezil, a drug for Alzheimer's disease. *Exp Gerontol* **40**:157–163.
Oh-hashi Y, Shindo T, Kurihara Y, Imai T, Wang Y, Morita H, Imai Y, Kayaba Y, Nishimatsu H, Suematsu Y, et al. (2001) Elevated sympathetic nervous activity in mice deficient in alphaCGRP. *Circ Res* **89**:983–990.
Okajima K and Harada N (2006) Regulation of inflammatory responses by sensory neurons: molecular mechanism(s) and possible therapeutic applications. *Curr Med Chem* **13**:2241–2251.
Okajima K and Harada N (2008) Promotion of insulin-like growth factor-I production by sensory neuron stimulation; molecular mechanism(s) and therapeutic implications. *Curr Med Chem* **15**:3095–3112.
Palmer TD, Willhoite AR, and Gage FH (2000) Vascular niche for adult hippocampal neurogenesis. *J Comp Neurol* **425**:479–494.
Ramsey MM, Adams MM, Ariwodola OJ, Sonntag WE, and Weiner JL (2005) Functional characterization of des-IGF-1 action at excitatory synapses in the CA1 region of rat hippocampus. *J Neurophysiol* **94**:247–254.
Ryan SH, Williams JK, and Thomas JD (2008) Choline supplementation attenuates learning deficits associated with neonatal alcohol exposure in the rat: effects of varying the timing of choline administration. *Brain Res* **1237**:91–100.
Sakurai O and Kosaka T (2007) Nonprincipal neurons and CA2 pyramidal cells, but not mossy cells are immunoreactive for calcitonin gene-related peptide in the mouse hippocampus. *Brain Res* **1186**:129–143.
Sidman RL, Angevine JBJ, and Pierce ET (1977) *Atlas of the Mouse Brain and Spinal Cord*. Harvard University Press, Cambridge, MA.
Sugimoto H, Ogura H, Arai Y, Limura Y, and Yamanishi Y (2002) Research and development of donepezil hydrochloride, a new type of acetylcholinesterase inhibitor. *Jpn J Pharmacol* **89**:7–20.
Suzuki R, Morcuende S, Webber M, Hunt SP, and Dickenson AH (2002) Superficial NK1-expressing neurons control spinal excitability through activation of descending pathways. *Nat Neurosci* **5**:1319–1326.
Tei E, Yamamoto H, Watanabe T, Miyazaki A, Nakadate T, Kato N, and Mimura M (2008) Use of serum insulin-like growth factor-I levels to predict psychiatric non-response to donepezil in patients with Alzheimer's disease. *Growth Horm IGF Res* **18**:47–54.
Tie-Jun SS, Xu Z, and Hökfelt T (2001) The expression of calcitonin gene-related peptide in dorsal horn neurons of the mouse lumbar spinal cord. *Neuroreport* **12**:739–743.
Trejo JL, Llorens-Martín MV, and Torres-Alemán I (2008) The effects of exercise on spatial learning and anxiety-like behavior are mediated by an IGF-I-dependent mechanism related to hippocampal neurogenesis. *Mol Cell Neurosci* **37**:402–411.
Vignery A and McCarthy TL (1996) The neuropeptide calcitonin gene-related peptide stimulates insulin-like growth factor I production by primary fetal rat osteoblasts. *Bone* **18**:331–335.
Watanabe T, Miyazaki A, Katagiri T, Yamamoto H, Idei T, and Iguchi T (2005) Relationship between serum insulin-like growth factor-1 levels and Alzheimer's disease and vascular dementia. *J Am Geriatr Soc* **53**:1748–1753.
Winblad B, Kilander L, Eriksson S, Minthon L, Båtsman S, Wetterholm AL, Jansson-Blixt C, and Haglund A (2006) Donepezil in patients with severe Alzheimer's disease: double-blind, parallel-group, placebo-controlled study. *Lancet* **367**:1057–1065.
Ye P, Popken GJ, Kemper A, McCarthy K, Popko B, and D'Ercole AJ (2004) Astrocyte-specific overexpression of insulin-like growth factor-I promotes brain overgrowth and glial fibrillary acidic protein expression. *J Neurosci Res* **78**:472–484.

Address correspondence to: Dr. Kenji Okajima, Department of Translational Medical Science Research, Nagoya City University Graduate School of Medical Sciences, Kawasumi 1, Mizuho-cho, Mizuho-ku, Nagoya 467-8601, Japan. E-mail: whynot@med.nagoya-cu.ac.jp

Seminars in Cell & Developmental Biology 21 (2010) 301–308

Contents lists available at ScienceDirect

Seminars in Cell & Developmental Biology

journal homepage: www.elsevier.com/locate/semcdb

Review

Evolving maps in craniofacial development

Yorick Gitton[a,1], Églantine Heude[a,1], Maxence Vieux-Rochas[a,2], Laurence Benouaiche[a,b], Anastasia Fontaine[a], Takahiro Sato[c], Yukiko Kurihara[c], Hiroki Kurihara[c], Gérard Couly[a,b], Giovanni Levi[a,*]

[a] Évolution des Régulations Endocriniennes, CNRS UMR 7221, Muséum National, d'Histoire Naturelle, 75231 Paris Cedex 05, France
[b] Service de Chirurgie Plastique, Maxillofaciale et Stomatologie, Hôpital Necker-Enfants Malades, 149, rue de Sèvres, 75015 Paris, France
[c] Department of Physiological Chemistry and Metabolism, Graduate School of Medicine, University of Tokyo, 7-3-1 Hongo, Bunkyo-ku, Tokyo 113-0033, Japan

ARTICLE INFO

Article history:
Available online 18 January 2010

Keywords:
Craniofacial
Neural Crest
Endoderm
Endothelin-1
Mesoderm

ABSTRACT

The shaping of the vertebrate head results from highly dynamic integrated processes involving the growth and exchange of signals between the ectoderm, the endoderm, the mesoderm and Cephalic Neural Crest Cells (CNCCs). During embryonic development, these tissues change their shape and relative position rapidly and come transiently in contact with each other. Molecular signals exchanged in restricted regions of tissue interaction are crucial in providing positional identity to the mesenchymes which will form the different skeletal and muscular components of the head. Slight spatio-temporal modifications of these signalling maps can result in profound changes in craniofacial development and might have contributed to the evolution of facial diversity. Abnormal signalling patterns could also be at the origin of congenital craniofacial malformations. This review brings into perspective recent work on spatial and temporal aspects of facial morphogenesis with particular focus on the molecular mechanisms of jaw specification.

Contents

1. Plasticity and regenerative potential of CNCCs

The contribution of Cephalic Neural Crest Cells (CNCCs) to head development was initially recognized by Wilhelm His, Sr. while studying the development of olfactory structures of the chick neurula [1]. He coined the term 'Zwischenstrang' (German for 'Middle chord') to describe a transient, rapidly moving, cell contingent ingressing between the primary germ layers.

The formation of head cartilages and bones was long considered as a mesodermal fate. Yet, as soon as 1893, shortly after Neural Crest Cells (NCCs) were described, Platt demonstrated their contribution to facial chondro-skeletogenesis [2,3]. However, it took more than five decades for this concept to be accepted [4].

Abbreviations: CNCCs, Cephalic Neural Crest Cells; CPM, cranial paraxial mesoderm; Edn1, Endothelin-1; Ednra, Endothelin-1 receptor type A; Mc, Meckel's cartilage; NCCs, Neural Crest Cells; OAVS, oculo-auriculo-vertebral spectrum; PA1, PA2, pharyngeal arch 1,2; pq, palatoquadrate; RA, retinoic acid; RAEs, retinoic acid embryopathies; SpM, lateral splanchnic mesoderm.

* Corresponding author at: UMR 7221 CNRS/MNHN, 7, rue Cuvier, 75005 Paris, France. Tel.: +33 1 40793621; fax: +33 1 40793621.
E-mail address: glevi@mnhn.fr (G. Levi).
[1] These authors have equally contributed to this paper.
[2] Present address: National Research Center Frontiers in Genetics, School of Life Sciences, Ecole Polytechnique Fédérale (EPFL), Lausanne, Switzerland.

1084-9521/$ – see front matter © 2010 Elsevier Ltd. All rights reserved.
doi:10.1016/j.semcdb.2010.01.008

Cell lineage experiments led initially to an over-representation of fate restriction of CNCCs in head morphogenesis supporting the view that pre-migratory CNCCs are irreversibly restricted in their topographic and tissular fate [5]. It took extensive transplantation experiments to challenge this 'neural-crest pre-patterning model', leading to the consensus view that while early target territories are assigned to pre-migratory CNCCs, these cells retain until late stages of migration the capacity to alter their specification according to local signals [6,7].

The fact that CNCCs exhibit a large repertory of differentiated phenotypes which can be individually induced by external factors [8], supported the notion that late events determine head morphogenesis.

Now considered the 'fourth' germ layer [9], NCCs can be seen as an embryonic stem cell reserve which, in the head, contributes to the formation of most chondro- and dermatocranial elements and other connective tissues (for reviews see for example [10,11]).

Possibly, the most interesting characteristic of CNCCs is their high level of plasticity [12]. While truncal Neural Crest Cells maintain an irreversible memory of their rostro-caudal origin [13], CNCCs have the remarkable capacity to substitute for one-another and replace missing cellular contingents until late in neurulation.

The plasticity of CNCCs is so extensive that drastic bilateral extirpation of the neural folds from the prosencephalic to the anterior rhombomeric level can be completely rescued by grafting small fragments of CNCCs presumptive territory [14–20]. Independently from their anterior–posterior origin within the prosencephalic/rhombomeric neural plate, these small contingents of CNCCs proliferate and finally give rise to apparently normal craniofacial structures. The capacity to replace missing contingents of CNCCs is, however, limited to cells deriving from anterior *Hox*-negative territories. Hox-positive truncal NCCs cannot compensate for missing CNCCs. Actually, *Hox* gene expression precludes any engagement into the chondroskeletogenic lineage which remains a peculiarity of CNCCs [21]. Remarkably, *Hox* gene expression appears to be repressed by molecular signals produced by pharyngeal arch cells [22]. The central questions to understand the origin of cephalization could well be how the anterior limit of *Hox* gene expression has appeared during craniate evolution and how, then, the *Hox*-negative domain has expanded [23,24].

As, before delamination, *Hox*-negative CNCCs deriving from different anterior territories can substitute for each other, they are considered as a 'group of equivalence' [15].

How is CNCC plasticity maintained late in neurulation? To answer this question, the fate of CNCCs was monitored in function of their emigration timepoint by substitutive transplantations of presumptive mesencephalic CNCCs [25]. Collectively, these data led to propose that, upon completion of migration, a signal from leader CNCCs prevented further colonization by trailer cells. While the molecular nature of this interaction remains unknown, live cell tracings provides valuable insight showing direct physical interactions among chains of migratory CNCCs [26].

2. Short-distance interactions involved in shaping the head

Transplantation of small territories of the endoderm deriving from different rostro-caudal levels induce outgrowth of ectopic cartilages and associated bony elements [16,27]. Remarkably, the morphology of these structures displays characteristic features of either nasal, jaw or throat cartilages, depending upon the rostro-caudal origin of the endodermal graft. It appears therefore, that regionalized endodermal cues can direct CNCCs towards a specific morphogenetic pathway and that a map of the facial skeleton is inscribed in the endoderm. For example, surgical deletion and/or grafting experiments of the ventral part of the rostral-most endoderm of the avian neurula have shown that this territory is necessary and sufficient to instruct CNCCs to form the mesethmoid which is the ventral cartilage of the nasal capsule. This specific patterning interaction is mediated through the Sonic Hedgehog (Shh)-*Gli1* signalling pathway [27]. Interestingly, this interaction appears to be triggered by the arrival of CNCCs, which induce a strong increase in endodermal *Shh* expression. Similarly, *Fgf8* induction by incoming CNCCs had been considered a triggering event in craniofacial patterning [16,27]. One important question is how these interactions are maintained during the simultaneous migration of CNCCs and both the growth and displacement of endodermal territories. Indeed, the foregut endoderm builds as a continuous rolling-mat as more extra-embryonic materials gets engulfed from lateral and posterior fields [28–30]. The endoderm then elongates rostrally as new territories form ('endodermal zones' [27]).

Patterning of CNCCs depends as well upon cues from ectodermal cells. For example, in the frontonasal process, postmigratory CNCCs organize around developing olfactory pits and receive instructions to build nasal cartilages and bones. This homing site behaves as an organizer involving Fgf, Bmp and Wnt signalling [31].

Which molecular cues are instructing CNCCs towards their morphogenetic program and how a signalling map is generated in cephalic epithelia are, therefore, central questions to understand head morphogenesis. Mutational analysis in zebrafish has provided several candidate genes for endoderm-derived instructive cues in craniofacial patterning (see for instance [32]). Among those, signalling cascades involving Shh, Fgf, Wnt and Bmp have been shown to be involved in the control of CNCCs migration, survival, apoptosis, tissue-specific terminal differentiation and patterned structural arrangement. As these results have been recently reviewed [33,34], we will focus here on the involvement of Endothelin-1 (Edn1) signalling in defining patterning maps as this pathway has not, so far, received as much attention as others.

3. Endothelin-1-dependent activation of *Dlx* genes and the specification of jaw identity

Although the nature of signals involved in instructing CNCCs remains still to be completely elucidated, evidence suggests that Fgfs, Bmps, Edn1 and Shh are surely involved [27,35,36]. In particular, Edn1 signalling plays a pivotal role for the specification of jaw identity: in its presence a lower jaw is formed; in its absence only maxillary structures are generated. Loss of Edn1 → Ednra (Endothelin-1 receptor type A) signalling results in the downregulation of *Dlx5* and *Dlx6*, leading to the transformation of lower into upper jaw structures similar to that observed after the double inactivation of these genes [37–40]. Conversely, the constitutive activation of *Ednra* induces the transformation of maxillary into mandibular structures with duplicated Meckel's cartilages and dermatocranial jaws constituted by four opposing dentary bones [41] (Fig. 1). A similar transformation is obtained by forcing the expression of *Hand2*, a downstream target of the Edn1 pathway, in the *Ednra* domain. These skeletal transformations are accompanied by neuromuscular remodelling with either the absence or duplication of the masseter muscle. Thus, within the first pharyngeal arch (PA1), CNCCs are competent to form both mandibular and maxillary structures and an Edn1 switch is responsible for the choice of either morphogenetic program.

It is interesting to observe that the effects of Ednra constitutive activation are mostly restricted to PA1 despite the fact that *Ednra* is broadly expressed by the CNCC-derived ectomesenchyme including, for example, the frontonasal prominence. This suggests that the competence to respond to Edn1/Ednra signalling is limited to a sub-

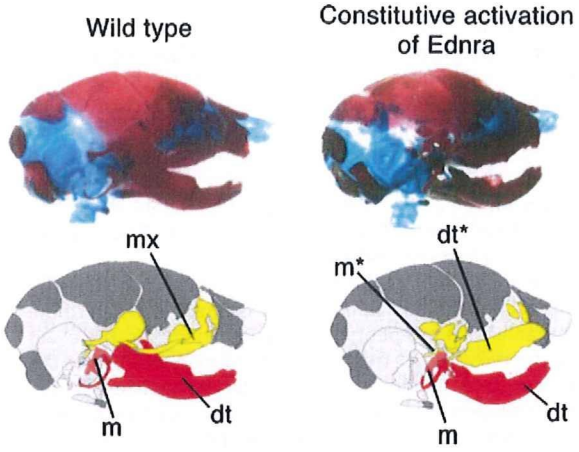

Fig. 1. Constitutive activation of Ednra results in the transformation of maxillary into mandibular structures. Representative images and schematic drawings of the dermatochranium of E18.5 normal and mutant mice in which the endothelin receptor A is constitutively activated. Note the transformation of the maxillary arch into a duplicated dentary bone with duplication of the malleus. *Abbreviations:* dt, dentary; dt*, duplicated dentary; m, malleus; m*, duplicated malleus; mx, maxillary arch. Adapted from [41].

population of *Hox*-negative CNCCs which begins to individualize already during early migration [35,40–45].

Vertebrate *Dlx* genes, targets of Edn1 signalling, are characterized by a homeobox homologous to that of *Drosophila distalless* (*dll*) [46–48]. In the mouse and human genome, there are six *Dlx* genes organized in three bigenic clusters *Dlx1–Dlx2*, *Dlx3–Dlx4* and *Dlx5–Dlx6*. Within PA1 of mouse embryos at 10.5 days of development (E10.5), *Dlx* genes are expressed in nested proximo/distal domains: *Dlx1* and *Dlx2* in the proximal and distal maxillary and mandibular prominences, *Dlx5* and *Dlx6* in the entire mandibular prominence, while *Dlx3* only in a medio/distal territory of the mandibular prominence [38,49]. The most informative data on the role of *Dlx* genes in PA1 patterning come from the analysis of mice carrying single or multiple inactivating mutations for *Dlx1*, *Dlx2*, *Dlx5* and *Dlx6*. In *Dlx5;Dlx6* double mutant mice, lower jaw cartilages and bones are transformed and acquire the shape typical of upper jaw elements. Furthermore, in *Dlx5;Dlx6* double mutant mice, vibrissae and palatine rugae are symmetrically present in the upper and lower jaw suggesting that an homeotic transformation has taken place [37,38]. In *Dlx1;Dlx2* double mutant mice the proximal maxillary region develops abnormal skeletal elements reminiscent of the reptilian upper jaw [50,51].

These observations have led to the suggestion that the combinatorial expression of *Dlx* genes by PA1 CNCCs determine their relative position and their capacity to form different skeletal elements [49,50,52].

Several genes have been shown to act downstream of *Dlx5* and *Dlx6*, including *Gsc*, *Pitx1*, *Wnt5a*, *Dlx3*, *Meis2*, and the bHLH transcription factor *Hand2* [37,38,49,53]. A further set of candidate targets of Dlx5/6 have been recently identified by gene expression profiling of *Dlx5;Dlx6* double null mandibular arches [54]. Several of these genes might be direct targets of Dlx5/6 (e.g. *Gbx2*, *Hand2*) as their promotors harbour Dlx-binding regulatory elements [54,55].

In order to dissect the regulatory events which govern PA1 patterning, many studies have analyzed the effect of either loss-of-function [35,37,38,41,43,53,56–59] or gain-of-function mutants [41]. These genetic experimental settings, however, cannot discriminate between early and late regulatory events.

We recently gained insight into the dynamics of PA1 patterning, by providing quantitative data on the effects of allelic reduction of *Edn1* and *Dlx5;Dlx6* at different developmental stages (Vieux-Rochas, unpublished observations). Our findings are complementary to those recently reported by Ruest and Clouthier [60] using Neural Crest Cell-specific gene deletion and receptor antagonism, and corroborate and extend their major conclusions.

We show that, during PA1 development, different Edn1-dependent regulatory pathways act at diverse developmental times in distinct regions of PA1. At early stages of development, up to E9.5 during CNCCs colonization, Edn1 signalling activates *Dlx5/6* expression in CNCCs [35,42]. At later stages, diverse regulations take place in different regions of PA1: in the most proximal part *Dlx5/6* are activated independently from Edn1 and their expression is not associated to *Gsc* activation. More distally *Dlx5/6* activation depends from Edn1 signalling and results in the upregulation of downstream genes including *Gsc* and *Pitx1*.

The nested *Dlx* gene expression pattern should be viewed as the final result of a highly dynamic process, as by E10.5 most CNCCs have migrated to their final position in PA1, have initiated expression of PA-specific genes and are already fate-committed [12,19,61]. The "hinge and caps" architectural and signalling organization of the E10.5 PA1 (proposed in [62]) is likely to be the consequence of patterning events occurring at much earlier stages.

An interesting point is the sensitivity of the proximal part of PA1 to variations in the genetic environment. Indeed, inactivation or allelic reductions of *Edn1*, *Ednra*, *Dlx5* [53,56], *Dlx6* [54], *Gsc* [63], *Pitx1* [64,65], *Gbx2* [66] all show proximal defect of the dentary or of the middle and external ear whereas derivatives of the distal part of the first arch are not affected.

4. Retinoic acid treatment to study the dynamics of signalling to CNCCs

Retinoic acid (RA), the active metabolite of vitamin A, is essential for normal development of most vertebrate species. RA can also act as a potent teratogen if it is administered during embryonic development in all vertebrates and even in certain invertebrates [67–69]. The malformations induced by RA treatment are very different depending on the dose administered and on the developmental stage at the time of exposure [67–69]. Oral intake of RA during the first weeks of human pregnancy results in highly variable morphological fetal lesions collectively named "Retinoic Acid Embryopathies" (RAEs); these often include severe defects of the jaws and of the middle and external ear [70–73]. Treatment of pregnant mice or of cultured mouse embryos with RA at E8.0 induces fusion and hypoplasia of PA1 and PA2. As most of the structures affected by RA treatment derive from PA1 and PA2, which are colonized by incoming CNCCs [16,24,74–78], it has been repeatedly suggested that CNCCs could be the primary target of RA-induced teratogenesis of facial structures [79–83]. This notion is derived from the fact that most dysmorphic structures in RAE are CNCCs derivatives and was reinforced by initial analyses of animal models suggesting that excess RA could alter CNCC survival and migration [84,85].

However, it has been shown that retinoid-induced defects of PA1 and PA2 occur without any obvious alteration of CNCC migration or apoptosis [80]. More importantly, the RA-mediated transduction machinery is not active in CNCCs shortly after their arrival in the PAs [86]. This notion is further supported by reports showing that CNCCs, although expressing certain RA nuclear receptors [87], may not respond directly to RA under physiological conditions [88–91]. Therefore, CNCCs do not seem to be direct targets of RA.

As mentioned above, grafting and fate mapping experiments have unequivocally shown that molecular signals deriving from the endodermal and ectodermal epithelial linings of PA1, are essential